

**Design and Development  
of Microporous Ti-35Nb-5Ta-7Zr Alloy  
and its Characterization**



**By  
Sohaib Ahmad**

**School of Chemical and Materials Engineering  
National University of Sciences and Technology  
2023**

# **Design and Development of Microporous Ti-35Nb-5Ta-7Zr Alloy and its Characterization**



Name: Sohaib Ahmad

Reg. No: 00000317690

**This thesis is submitted as a partial fulfillment of the requirements  
for the degree of**

**MS (Materials and Surface Engineering)**

**Supervisor Name: Dr. Khurram Yaqoob**

**School of Chemical and Materials Engineering (SCME)  
National University of Sciences and Technology (NUST)  
H-12 Islamabad, Pakistan**

**April 2023**



### THESIS ACCEPTANCE CERTIFICATE

Certified that final copy of MS thesis written by **Mr Sohaib Ahmad** (Registration No 00000317690), of School of Chemical & Materials Engineering (SCME) has been vetted by undersigned, found complete in all respects as per NUST Statues/Regulations, is free of plagiarism, errors, and mistakes and is accepted as partial fulfillment for award of MS degree. It is further certified that necessary amendments as pointed out by GEC members of the scholar have also been incorporated in the said thesis.

Signature: \_\_\_\_\_

Name of Supervisor: Dr Khurram Yaqoob

Date: \_\_\_\_\_

31/08/2023

Signature (HOD): \_\_\_\_\_

Date: \_\_\_\_\_

31/08/2023

Signature (Dean/Principal): \_\_\_\_\_

Date: \_\_\_\_\_

4.9.2023



Form TH-1

(Must be type written)

National University of Sciences & Technology (NUST)  
MASTER'S THESIS WORK  
Formulation of Guidance and Examination Committee (GEC)

Name: Sohaib Ahmad NUST Regn No: 317690

Department: Materials Engineering

Specialization: MS in Materials & Surface Engineering

Credit Hour Completed: 9 24 CGPA: 3.69 ✓

Course Work Completed

S/No	Code	Title	Core/Elective	CH	Grade
1	MSE 811	Material Thermodynamics	Core	3	(A) B+
2	MSE 821	Mechanical Behaviour of Materials	Core	3	(B+) A
3	MSE 882	Corrosion and control Engg	Elective	3	B+
4	MSE 812	Phase transformation & microstructure	Core	3	A
5	MSE 851	Surface engineering & characterization	Core	3	B+
6	MSE 861	Engineering ceramics & glasses	Elective	3	A
7	MSE-981	Manufacturing processes	Elective	3	B+
8	MSE-852	Advance surface coating	Elective	3	B+

Date 4-6-2021  
9 RM-890 Research methodology

Student's Signature Sohaib

Exam B+  
04/6/21

Thesis Committee

- Name: Dr. Khurram Yaqoob (Supervisor) Signature: [Signature]  
Department: Materials Engineering
- Name: \_\_\_\_\_ (Co-Supervisor, if appointed) Signature: \_\_\_\_\_  
Department: Materials Engineering
- Name: Dr. Usman Iqat Signature: \_\_\_\_\_  
Department: Materials Engineering
- Name: Dr. Muhammad Irfan Signature: \_\_\_\_\_  
Department: Materials Engineering
- Name: \_\_\_\_\_ Signature: \_\_\_\_\_  
Department: \_\_\_\_\_

Date: 28/6/2021

Signature of Head of Department: [Signature]  
APPROVAL

Date: 30.6.2021

Dean/Principal [Signature]

Distribution

- 1x copy to Exam Branch, Main Office NUST
- 1x copy to PGP Dte, Main Office NUST
- 1x copy to Exam branch, respective Institute

School of Chemical and Materials Engineering (SCME) Sector H-12, Islamabad

FORM TH-4



National University of Sciences & Technology (NUST)

MASTER'S THESIS WORK

We hereby recommend that the dissertation prepared under our supervision by  
Regn No & Name: **00000317690 Sohaib Ahmad**

Title: Design and Development of Microporous Ti-35Nb-5Ta-7Zr alloy and its Characterization.

Presented on: 18 Aug 2023 at: 1500 hrs in SCME Seminar Hall

Be accepted in partial fulfillment of the requirements for the award of Masters of Science degree in **Materials & Surface Engineering**.

Guidance & Examination Committee Members

Name: Dr Usman Liaqat

Signature: 


Name: Dr Muhammad Irfan


Signature: 

Supervisor's Name: Dr Khurram Yaqoob

Signature: 

Dated: 28/8/23

  
Head of Department  
Date 28/8/23

  
Dean/Principal  
Date 31.8.2023

School of Chemical & Materials Engineering (SCME)

# **Dedication**

I dedicate this thesis to my parents, who have always supported me throughout my life and have stood by me through thick and thin, and to which I owe everything in this life.

## **Acknowledgement**

First and foremost, I would like to thank Allah Almighty for giving me the strength and opportunity to undertake this research study and to preserve and complete it satisfactorily. Without His blessings, this work would not have been possible.

I wish to express my sincere gratitude to my supervisor, Dr Khurram Yaqoob, who has been a tremendous mentor for me. I would like to thank him for his encouragement, enthusiastic supervision, and help during my research and for allowing me to grow as research scientist. I am also grateful to lab fellows and seniors for their support.

Finally, I would like to thank my family and friends for their unconditional support and encouragement. To the most important people in my life, my parents, my siblings, this research work could only be completed with your support foremost.

**Sohaib Ahmad**

Reg No. 00000317690

## Abstract

Ti-35Nb-5Ta-7Zr titanium alloy is a Beta phase titanium alloy with good mechanical, excellent corrosion resistance, and better biocompatible properties. This study is focused on introducing porosity in the Ti-35Nb-5Ta-7Zr alloy with the intent to produce porous alloy with a suitable combination of low elastic modulus and yield strength. Porous Ti-35Nb-5Ta-7Zr alloy was fabricated in argon arc melting and yttrium was added in different proportions, followed by a chemical dealloying process. The developed porous alloys were thoroughly investigated after synthesis, including microstructural, corrosion and mechanical characterization. A microstructure based on a matrix mainly composed of BCC beta phase and interdendritic areas consisting of yttrium phase was formed by adding yttrium in Ti-35Nb-5Ta-7Zr alloy. With increasing amounts of yttrium in Ti-35Nb-5Ta-7Zr alloy, the amount of interdendritic regions increased. An X-ray diffractometry (XRD) examination confirmed that yttrium was removed through dealloying process. SEM investigation of the generated porous alloys revealed the formation of interconnected porosity. The developed porous alloys were evaluated through mechanical and corrosion testing. The mechanical evaluation of the manufactured alloys exhibited a broad spectrum of mechanical properties. Developed porous alloys showed elastic modulus and yield strength in the range 29.5 Gpa to 13.7 Gpa, and 293.98 MPa to 215.12 MPa, respectively. The mechanical properties achieved in this study were in the within acceptable limits of human bone and are for biomedical applications. Corrosion resistance of porous alloys showed a decreasing trend with an increase in porosity.



# Table of Contents

<b>Chapter:1</b> .....	1
<b>1 Introduction:</b> .....	1
<b>1.1 Classification of biomaterials:</b> .....	2
<b>1.1.1 Polymers:</b> .....	2
<b>1.1.2 Ceramics:</b> .....	3
<b>1.1.3 Metallic implants:</b> .....	3
<b>1.2 Properties of biomaterials:</b> .....	4
<b>1.2.1 Biocompatibility:</b> .....	4
<b>1.2.2 Mechanical properties:</b> .....	4
<b>1.2.3 Wear and corrosion properties:</b> .....	5
<b>1.2.4 Surface topography:</b> .....	6
<b>1.3 Issues with implants:</b> .....	6
<b>1.4 Research Objective:</b> .....	7
<b>2 Literature Review:</b> .....	9
<b>2.1 Conventional Biomedical implants:</b> .....	9
<b>2.1.1 Stainless Steel:</b> .....	9
<b>2.2 Ti alloy:</b> .....	11
<b>2.2.1 Alloying chemistry: microstructure design</b> .....	11
<b>2.3 Classification and grading of titanium and its alloys:</b> .....	13
<b>2.3.1 Biocompatibility of alloying elements:</b> .....	14
<b>2.5 Biocompatibility of titanium alloys:</b> .....	15
<b>2.6 <math>\alpha</math> titanium alloys</b> .....	16
<b>2.7 <math>\alpha</math>-<math>\beta</math> titanium alloys:</b> .....	16
<b>2.8 <math>\beta</math> titanium alloys:</b> .....	18
<b>2.9 Stress shielding in implants:</b> .....	19
<b>2.9.1 Efforts to reduce elastic modulus:</b> .....	20

2.10 Our chosen alloy:.....	23
<b>3 Experimental Techniques .....</b>	<b>25</b>
3.1 Alloy preparation: .....	25
3.2 Grinding and polishing:.....	26
3.3 Dealloying: .....	27
3.4 Characterization of samples:.....	28
3.4.1 SEM: .....	28
3.4.2 X-ray diffraction (XRD):.....	30
3.5 Mechanical testing:.....	31
3.5.1 Compression:.....	31
3.5.2 Microhardness: .....	32
3.6 Wetting angle testing: .....	33
3.7 Electrochemical testing:.....	33
3.7.1 OCP:.....	34
3.7. 2 EIS:.....	35
<b>4 Results and discussion: .....</b>	<b>36</b>
4.1 Development of Ti-35Nb-5Ta-7Zr porous alloy:.....	36
4.2 Phase analysis: .....	37
4.3 Scanning electron microscopy:.....	38
4.4 Weight loss method: .....	41
4.5 Mechanical properties: .....	42
4.6 Wetting angle:.....	47
4.7 Corrosion Results: .....	48
4.7.1 Open Circuit Potential: .....	49
4.7.2 Potentiodynamic polarization:.....	49
4.7.3 Electrochemical impedance spectroscopy (EIS): .....	52

## List of Figures

<b>Figure 1</b> Hip implant, and (b) terminologies of involved components [2] .....	2
<b>Figure 2</b> Elastic modulus of biomedical implants. [2] .....	5
<b>Figure 3</b> Schematic of Stress shielding effect [26]. .....	6
<b>Figure 4</b> Revision procedures i.e., Pain, aseptic loosening, wear, and infection [28].	7
<b>Figure 5</b> Vacuum arc melting furnace.....	25
<b>Figure 6.</b> Solidified alloy button .....	26
<b>Figure 7</b> Mounting Machine and mount.....	26
<b>Figure 8.</b> Polishing Machine. ....	27
<b>Figure 9.</b> Working principle of SEM. ....	29
<b>Figure 10.</b> Scanning electron microscope setup.....	29
<b>Figure 11.</b> XRD working principle. ....	30
<b>Figure 12.</b> XRD equipment at SCME NUST.....	31
<b>Figure 13.</b> Alloy sample During compression testing.....	31
<b>Figure 14.</b> Universal testing machine at SCME NUST .....	32
<b>Figure 15.</b> Micro Vickers hardness testing machine .....	33
<b>Figure 16.</b> Gamry workstation for electrochemical testing.....	34
<b>Figure 17.</b> Pseudo binary phase diagram between Ti-35Nb-5Ta-7Zr and Yttrium ..	37
<b>Figure 18.</b> XRD pattern of (a) as-cast FC1 and de-alloyed FC1 (b) as-cast C2 and de-alloyed FC2 (c) as-cast C3 and de-alloyed FC34 (d) as-cast C4 and de-alloyed FC4.....	38
<b>Figure 19.</b> As cast SEM images of (a) C1, (c)C2, (e)C3, (g) C4,) and dealloyed (b)FC1 (d) FC2 (f) FC3 (h) FC4 .....	40
<b>Figure 20</b> EDX mapping of as cast C2.....	41
<b>Figure 21</b> Weight loss data of dealloyed samples. ....	42
<b>Figure 22</b> Compressive stress strain graphs of Dealloyed samples FC1 to FC4.....	43
<b>Figure 23</b> Comparison of Elastic modulus of bone with (a)elastic modulus (b) Yield stress.....	44
<b>Figure 24</b> Hardness pf developed porous samples. ....	45
<b>Figure 25.</b> Comparison Yield strength and Elastic modulus of Developed porous alloys with literature.....	46

<b>Figure 26</b> Contact angle of developed porous alloys. ....	47
<b>Figure 27</b> Contact angle Developed porous alloys (a)FC1 (b) FC2 (c) FC3 (d) FC4 .....	48
<b>Figure 28.</b> Open circuit potential vs time of developed porous alloys in hank's solution.....	49
<b>Figure 29.</b> Electrochemical results of Developed foams being exposed to Hank's solution.....	51
<b>Figure 30</b> Nyquist plot from Electrochemical Impedance of Porous Ti-35Nb-5Ta- 7Zr alloys .....	53
<b>Figure 31</b> Comparison of Ecorr and Icorr value of porous alloys in this study with literature. ....	54

## List of Tables

<b>Table 1.</b> Titanium and titanium alloys used in medical implants according to ASTM/UN standards.....	14
<b>Table 2</b> The important mechanical characteristics of titanium and titanium alloys designed for orthopedic implants [31]. .....	17
<b>Table 3</b> Various systems of Beta titanium alloys. ....	19
<b>Table 4</b> Elastic modulus of various Beta type alloys .....	21
<b>Table 5.</b> Enthalpy of mixing of elements selected for the system.....	36
<b>Table 6</b> Corrosion parameters calculated from polarization curves and EIS. ....	51

# Chapter:1

## Introduction

The usage of orthopedic implants becomes necessary when a patient demands them to fulfil specific medical needs. Prosthetic implants are becoming more common in healing and replacing damaged or impaired tissues. In medicine, orthopedic implants are important. An orthopedic implant is an artificially medical device used to stabilize a fractured bone part or a damaged joint. Particularly when the human part gets fractured, worn out, and find difficulty to perform function on their own, orthopedic implants help to alleviate problems, a hip implants is shown Fig.1. For a variety of reasons, including bone fractures, osteoarthritis, scoliosis, spinal stenosis, and persistent discomfort, they may need to be replaced. For instance, during the self-healing period, broken bones are stabilized by pins, rods, screws, and plates. [1] According to estimates, 90% of people around the world suffer from degenerative diseases in the age after 40, which are brought on by either excessive and prolonged loading or a lack of normal biological self-healing capacity [2-4]. Problems in musculoskeletal like arthritis affected almost (10 M) individuals and cost 5 billion dollars in the UK to medical assist patients [5, 6]. Broken bones are another significant factor in the need for an artificial implant. The failure of a bone can occurs in a variety of ways, including fully, partially, simply, and complexly. Annually reported bone fractures in the UK are around 1 million, with road traffic accidents accounting for about 21% of those fractures [7]. Any age group can get a bone fracture. Yet, fractures seem to occur most frequently in children and the elderly. The most frequent fracture in kids is a fractured forearm, and boys get fractures more often than girls do. The most prone age group is often that of adolescence, which increases the risk of fracture. Moreover, because of the rapid bone growth that occurs during adolescence, teenagers' bones are more prone to shattering. Due to osteoporosis the incidence of broken bones naturally rises with age [8]. As a result, the restoration time is probably going to get longer with age. Synovial joints that include hip, knee, and shoulder, are the most prevalent kinds of joints in the human body. Despite their complexity and fragility, these joints are quite capable of functioning in stressful situations. Their functionality

is due to the presence of synovial fluid in the joint area and the load-bearing connective tissue known as articular cartilage [9].

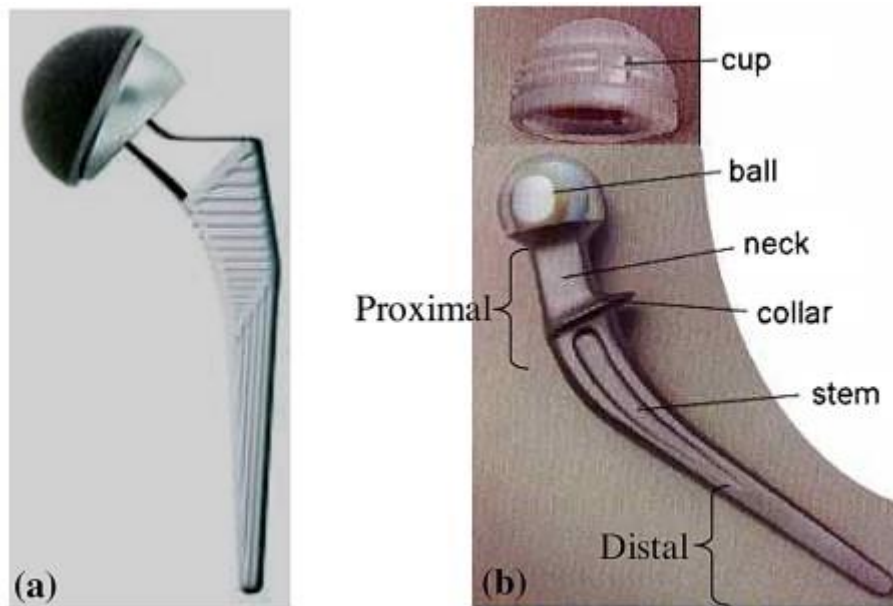


**Figure 1** Hip implant, and (b) terminologies of involved components [2]

The chronic conditions that may occur in these joints, such as arthritis, osteoarthritis, chondromalacia, and natural cartilage aging, can cause discomfort, stiffness, and even loss of function. Due to excess or the lack of a self-healing process, degeneration can result in a decline in the mechanical characteristics of bones. Surgery, such as arthroscopic surgery, is frequently needed to relieve discomfort and improve mobility in load-bearing joints that have degenerated. Diseased joints are replaced in this procedure with metal or plastic implants that are shaped appropriately [2,9].

## **1.1 Classification of biomaterials:**

Bio medical implants are classified as:

- Polymers
- Ceramics
- Metallic

### **1.1.1 Polymers:**

Polymers are the practical materials used in cardiovascular devices to substitute and promote the growth of different soft tissues. Many different polymeric materials have

been implanted in patients. These biomaterials found in applications, such as tissue adhesives, contact lenses, intraocular lenses, fixtures for extracorporeal oxygenators, and in dialysis [10]. The characteristics of polymers are determined by the mix, organization, and structure of their constituent macromolecules [11]. Additionally, the ability to adapt in many applications demands the synthesis of polymers with acceptable physicochemical, interfacial, and biomimetic qualities to fulfil specific purposes. These polymers must be prepared in various structures and compositions. Polymers have the advantages of being process easily with required mechanical properties in low cost. Synthetic and natural polymers are of two types that are used in field of medical. Few examples of synthetic polymer are acrylics, polyamides, polyesters, polyethylene, polysiloxanes, and polyurethanes. Although synthetic polymers are easily processed, their main drawback is that they are typically not biocompatible, which means that using them is frequently accompanied by inflammatory reactions [12].

### **1.1.2 Ceramics:**

A different class of materials is being used to design biomaterials: ceramics. The driving force for the use of ceramics in implants is due to their inertness, porous structure with high wear and compressive properties. Ceramics have been utilized in the development of diverse medical devices such as cardiac valves, artificial hip, knees, and dental implants, and also in the creation of implants for the middle and orbital ear. Ceramics are used to create biomaterials, but they are less frequently used than either metals or polymers. Ceramics' brittleness and low tensile strength in certain conditions severely limit their applications. However, bio ceramics of phosphates are frequently utilized to make perfect biomaterials because they are biocompatible and more bioactive [13].

### **1.1.3 Metallic implants**

Metallic implants have long been of great importance in the realm of the medical field. The utilization of metallic implants is of significant importance in human anatomy. Several joint and dental implants are fabricated from metals the examples for such implants include artificial dental and hip implants, screws, synthetic pacemakers, and orthodontic devices [11].



Engineers have identified metals as a paramount material for fabricating biomaterials, despite the existence of several other material options. Metallic-based implant materials for biomedical purposes are primarily influenced by their exceptional biocompatibility, pragmatic mechanical features, remarkable corrosion resistance, and economic viability [14].

## **1.2 Properties of biomaterials:**

The optimal choice of biomaterials for specific biomedical applications relies on several key considerations, including surface chemistry and morphology, non-toxicity, biodegradability, mechanical properties, and resistance to corrosion or wear [15].

### **1.2.1 Biocompatibility:**

The implant material's surface properties determine biocompatibility. Biomaterials should have surface that is free from toxicity and stable for prolonged time without generating allergic and inflammatory reactions. The biocompatibility of a substance is determined by the extent to which it can survive an acceptable host response in a particular circumstance, such as during implant surgery [16].

### **1.2.2 Mechanical properties:**

An implant that is intended to bear loads ought to exhibit distinct and remarkable mechanical attributes. The essential characteristics encompassed within this context are comprised of physical properties that includes high strength, elongation, low elastic modulus, high hardness and fatigue resistance. The implant's longevity is profoundly influenced by two key characteristics, namely, elastic modulus and fatigue strength, among the others. The advancement in implant materials comprising modulus of elasticity within the proximity of bone has earned significant consideration. (10-30 GPa). Numerous research has shown how a high elastic modulus might lead to an implant's limited lifespan. Due to the phenomenon of "Stress Shielding," there arises a non-uniform distribution of loads between the implanted structure and the bone. This, in turn, poses a challenge when there exists a significant difference of modulus between implant and bone. An early failure of implant may occur due to bone resorption and loosening of implants. [2,17–19]. Additionally, the material recommended in high load-bearing conditions needs to have a very high fatigue strength to endure repeated cyclic loading while in service. This may result in a buildup

of plastic distortion, which could spark the initiation of fatigue cracks at the implant's surface and early failure [20]. To increase the durability and life of the implant and preclude any further necessary surgeries, a biomaterial possessing a blend of superior mechanical characteristics and a reduced elastic modulus is imperative. Fig. 2 shows the wide range of elastic modulus of alloys.

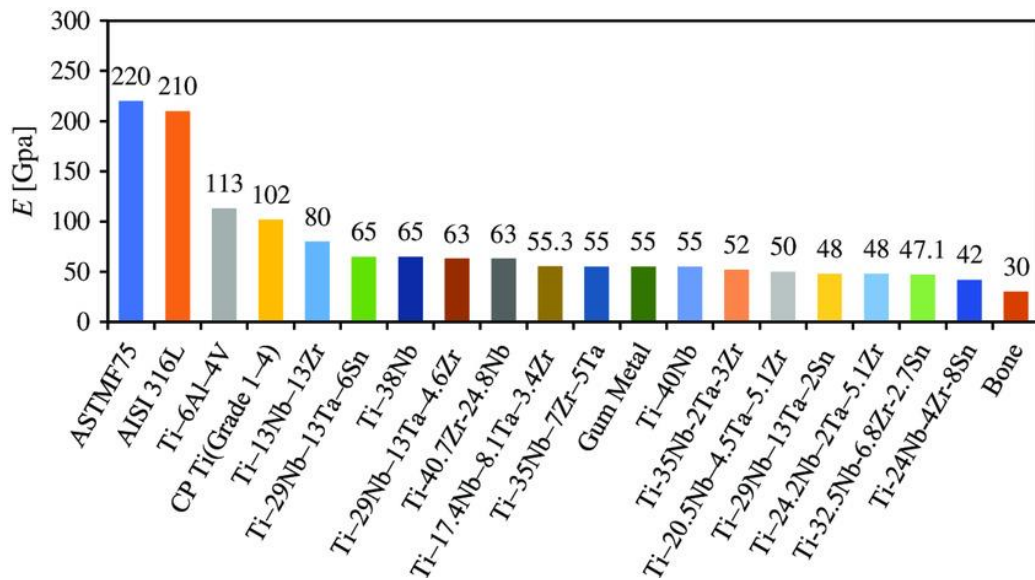


**Figure 2** Elastic modulus of biomedical implants. [2]

### 1.2.3 Wear and corrosion properties:

The implant's material must be corrosion- and wear-resistant; otherwise, ions from the implant might leak into human fluids and cause harmful and allergic reactions. The implant's resistance to wear and abrasion is used to estimate how long it will last. Poor wear resistance properties can lead to implant loosening, severe discomfort, and functional loss. If the implant is constantly rubbing against the surrounding bone, debris may accumulate when the wear and abrasive characteristics are poor. The debris that is subsequently created interacts with bodily tissues in an unfavorable way, leading to undesirable tissue reactions and, in some way, causing an implant to become loose. Therefore, an implant material should have exceptional wear properties in addition to the aforementioned properties [2].

### 1.2.4 Surface topography:

To increase surface area and allow for larger-scale contact with cells and tissues, a nano-porous architecture with interconnected pores of specified size is required. The impact of porosity is beneficial for adhesion of cells, proliferation, and osteogenesis. The important factors in the proliferation of new tissue and cells ingrowths around implants are roughness and chemistry of implants surface [21].

### 1.3 Issues with implants:

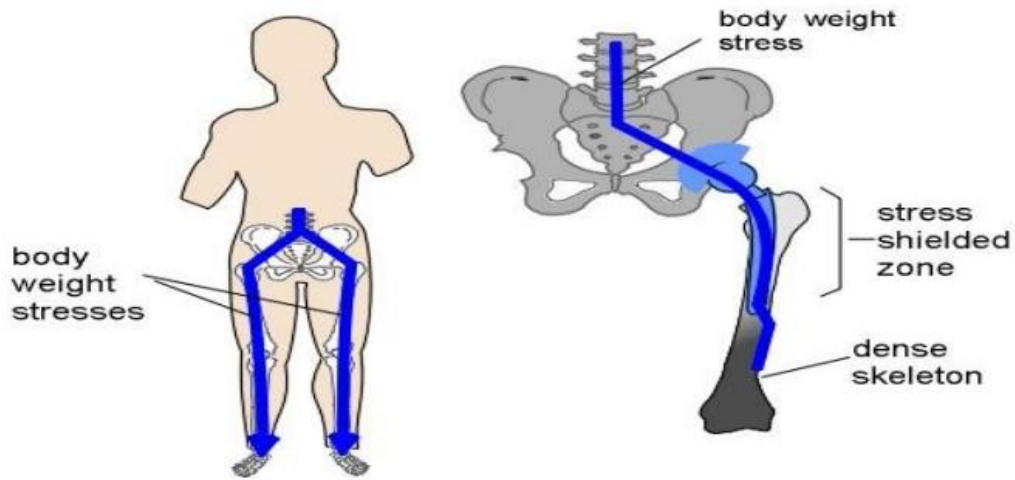


**Figure 3** Schematic of Stress shielding effect [26].

Implants made of metal have a higher fatigue strength than those made of other materials. Because of their high mechanical strength, they are also a suitable and desirable material for high loading applications, but metallic implants also have a higher modulus than bone. A higher implant modulus prevents the uniform delivery of the required stress to the adjacent bone, which weakens newly created bone, causes bone resorption, and deteriorate bone cells [22–24]. Stress shielding is a factor that contributes to implant loosening. When a bone implant removes common stresses from the bone, it might cause osteopenia, which is known as stress shielding; a schematic is presented in Fig. 3. The Wolff's law explains that bone in the body will remold itself against a response to loads that are applied to it [25]. A bone will therefore become less dense and weaker if the strain on it decreases because there will not be any stimulation for the ongoing remodeling needed to maintain bone density [26–29].

As illustrated in Fig .4, there are numerous causes of orthopedic implant failure. In the study by Havelin et al. [16], the failure mode for implants is loosening, which happens

when the implant moves or migrates within the bone or cement. Among the revision surgeries from 1987 to 1990 in Norway, loosening of implants accounted for 64% in 1993. Additionally, Malchau et al. [28] discovered that from 1987 to 1990 in Sweden, 79% of revisions occurred on by implant loosening. Furthermore, an analysis by the National joint research in UK in 2016 found that implant loosening accounted for 32.6% of all failure causes.

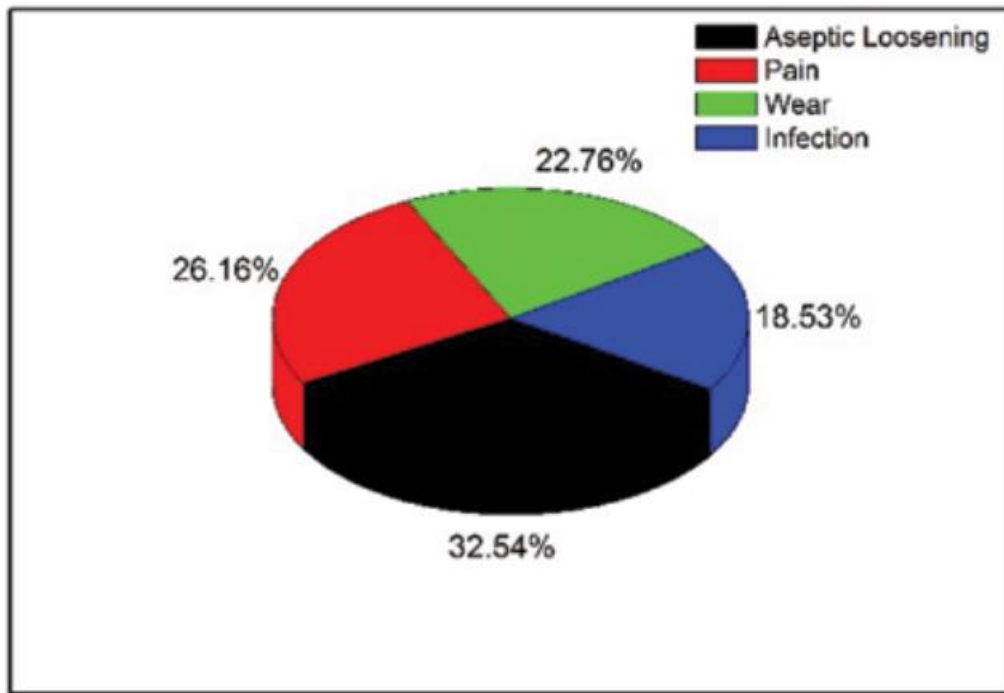


**Figure 4** Revision procedures i.e., Pain, aseptic loosening, wear, and infection [28].

#### 1.4 Research Objective:

The research objective for Ti-35Nb-5Ta-7Zr is formulated as follows:

- Designing of beta phase Ti-35Nb-5Ta-7Zr alloy using thermos Calc software to construct the phase diagram after studying the enthalpy mixing of the alloying elements.
- Development of alloy in arc melting furnace.
- To better understand the phase composition, and distribution of alloying elements in as-castTi-35Nb-5Ta-7Zr alloy, characterize its microstructure using SEM and XRD.

- Introduction of porosity in the Ti-35Nb-5Ta-7Zr alloy in different percentages through selective phase dissolution to achieve lower elastic modulus and characterization of resulted porous alloys through SEM and XRD.
- Evaluate of porous Ti-35Nb-5Ta-7Zr alloy in terms of mechanical properties, that contain hardness, yield strength and elastic modulus to determine its suitability for load-bearing applications.
- To investigate electrochemical properties (corrosion resistance) in order to better understand possible uses for it in the field of biomedical engineering.

# Chapter:2

## Literature Review

### 2.1 Conventional Biomedical implants:

Conventional orthopedic implants play a crucial role in restoring mobility and function to patients with orthopedic conditions. These medical devices are used in procedures such as joint replacements, fracture fixation, and spinal surgeries. They are designed to provide stability, support, and alignment to the musculoskeletal system, helping patients regain their quality of life.

Orthopedic implants have undergone significant advancements over the years, with improvements in design, materials, and surgical techniques. Orthopedic implants, such as permanent prosthetic devices and temporary fixation tools, often utilize metallic materials due to their essential properties. Biocompatibility, Strength, ductility, fracture toughness, hardness, corrosion resistance, are among the fundamental requirement in load-bearing applications. This is especially important for total joint prosthesis and fracture fixation systems.

#### 2.1.1 Stainless Steel:

A broad term Stainless steel is used for many types of ferrous alloys with a high chromium content (11-30 wt%) and different concentrations of nickel and further classified into two categories on the basis of chemical composition: chromium and chromium-nickel types. On the basis of their specific microstructure, they are further divided into four categories: an austenitic, martensitic, ferritic, and duplex (a combination of austenitic and ferritic) [31]. Widely utilized types of stainless steel as implants are 316L SS and 316L VM alloys in biomedical applications. These metal combinations contain ions of iron, chromium, nickel, and molybdenum. The addition of chromium to these alloys provides the implants with protection against corrosion and causes passivation, which creates a protective oxide layer. The presence of low carbon in 316L prevents corrosion within the body fluids [6]. Austenitic stainless alloys persist in their extensive usage for implantation purposes, owing to their abundant accessibility, economically feasible nature, outstanding manufacturability, well-established biocompatibility, and remarkable durability. These steels offer the advantage of versatile mechanical property control, allowing for the optimization of

strength and ductility across a broad spectrum. However, stainless steel implants can corrode in the environment that contains chlorine ions. Roughly 90% of 316L stainless steel implant experience pitting corrosion, necessitating the application of ceramic coatings to inhibit corrosion. A different variety of stainless steel known as 316L VM has corrosion-inhibiting properties that make it particularly useful in the biomedical field. A study conducted Okazaki et al. on the usage of 20 metallic 316L SS implants as replacements for hip arthroplasty. After 13 years since the implants were placed, there was an escalated discharge of metallic ions in the bodily fluid, ultimately resulting in regional inflammation and ultimate detachment of the artificial joint implant. Stainless-steel implant failures have been documented, along with problems like surface cracking, crevice corrosion, pitting, crack initiation, and intergranular corrosion seen in thighs of patients. Crevice corrosion is also a significant factor in implant failure. A higher Young's modulus (200 Gpa) of Stainless steel than the bone, may lead in detachment eventually due to mismatch of elastic modulus. Austenitic stainless steel specifically 316L offer wear resistance that is comparatively low, and cause generation of wear debris that can trigger allergic reactions in the surrounding tissue. This is another factor limiting its use in permanent implants. Therefore, stainless steel is not suitable for long-term applications, particularly for permanent fracture fixation devices, but can be used temporary due to its advantages of being cost-effective, easily manufacturable, and applicable [32].

#### **2.1.1.1 Biocompatibility stainless steel:**

Iron serves as the main matrix element in the alloy known as 316L stainless steel, as standardized by ASTM F138. It is also possible to modify this alloy in a number of ways. The primary alloying elements present in 316L are nickel, Chromium molybdenum, and manganese. The concept of bioactivity in this context pertains to the release of these elements in the form of soluble ions or insoluble particles [33].

#### **2.1.2 Cobalt base alloys:**

Haynes introduced the development of the cobalt-molybdenum superalloy, which was named Stellite and primarily intended for aircraft engine applications [34,35, 36]. This alloy demonstrated superior strength at elevated temperatures and offered improved resistance against corrosion in comparison to alternative superalloys [37]. In the 1930s, medical implants began utilizing cobalt-based alloys for the first time [38]. The dental

alloy vitallium, a CoCrMo alloy, was initially employed in cast dental applications and later modified for orthopedic purposes during the 1940s. CoCr alloys exhibit corrosion resistance that surpasses stainless steels by a significant factor and boast exceptional mechanical properties [31]. Cobalt-chromium based alloys in terms of corrosion resistance surpass stainless steels, particularly in chloride rich environments. Chemical composition of these alloys makes them superior regarding corrosion resistance. The presence of a high chromium concentration in the alloy help in the development of a naturally protective oxide coating ( $\text{Cr}_2\text{O}_3$ ). [39, 40, 41, 42, 43].

Comparing cobalt alloys to cortical bone (20–30 GPa), the Young's modulus is very high (220–230 GPa). Over time, stress shielding occurs that weakens bone, deteriorates it, potentially leading to loosening, fracture and implant failure. The unwanted stress shielding, and abrasion particles due to mobilization may accelerate prosthesis failure. Nickel, chromium, and cobalt are among the hazardous components generated from cobalt-based alloys that are causing problems. These substances may increase inflammation and trigger allergic reactions in the body. [43].

## **2.2 Ti alloy:**

Titanium has a low density, about 60% that of iron and about 50% that of cobalt. By using alloying and deformation techniques, this extraordinary metal can be significantly strengthened. At about 885 °C, titanium goes through an allotropic transformation that causes it to change its phase from alpha to a BCC beta phase. On the basis of microstructure titanium alloys are characterized as: alpha alloys, near-alpha phase, alpha+beta phase, and beta alloys. These alloys of titanium have 50% lower elastic modulus around than stainless steels and cobalt based alloys. Ti exhibits remarkable specific strength and is low weight as compared to stainless steels and cobalt-chromium alloys and are being used as biomaterials owing to their moderate low modulus, excellent biocompatibility, and higher corrosion resistance. Its tribological characteristics, however, are rather inadequate. The appealing properties of (CP-Ti) and  $\alpha + \beta$  Ti-6Al-4V alloys, as well as the introduction of metastable beta alloys, have aided in their rapid incorporation in medical industry [31].

### **2.2.1 Alloy design**

In contrast to stainless steels and cobalt-based alloys, where alloying is primarily focused on improving corrosion resistance, the primary objective in designing titanium



alloys is to enhance their mechanical properties. This is because titanium, as the base element, already possesses excellent inherent corrosion resistance. The alloying elements have significant effects on transformation temperature in titanium between (HCP) and (BCC) phases. Due to their role in transformation temperature from alpha phase-to-beta phase, whether it is an increase or decrease, these components are categorized as stabilizing additives for either the alpha or beta phase. The transformation temperature rises as their amount in the alloy increases because of interstitial elements (C, O<sub>2</sub> and N), they act as stabilizers for the alpha phase. Hydrogen functions as strong beta stabilizer, causing a decrease in the transformation temperature as its solute content increases. Due to its high affinity towards oxygen and nitrogen, titanium offers difficulties that are unusual for other metals. In addition to oxidation, subjecting titanium to high temperatures in the presence of air causes surface hardening through solid solution because of the internal diffusion of oxygen and nitrogen. The fatigue resistance and malleability of titanium alloys are adversely affected by the presence of an exteriorly hardened region described as the alpha case. Therefore, it necessitates the removal of this layer by means of mechanical machining, and milling, prior to utilizing the alloy for implantation purposes [31].

The modification of titanium alloys' microstructure and characteristics depends substantially on incorporation of substitutional alloying components. Moreover, additional components (B, Ga, Ge, and the rare earth elements), also took part in the process of alpha stabilization. Aluminum serves as a powerful alpha stabilizer. It is important to note that they are much less soluble in solids than oxygen or aluminum. These elements aren't typically used as alloying components today [44].

The beta phase of titanium exhibits higher solubility for various elements compared to the alpha phase. Since beta stabilizers elements don't combine with titanium to generate intermetallic compounds, they are favored as alloying elements. These elements are frequently combined with one or more isomorphous beta elements in alloys, which is a common practice, providing beta phase stabilization and preventing or minimizing the development of intermetallic compounds. Such compounds may form during thermomechanical processing and heat treatment processes at elevated temperatures. [31]. The commonly utilized elements for stabilizing the beta phase include (V, Mo, Nb, Cr, Fe, and Si). These elements act as strong stabilizers for the beta phase and improve hardenability. Furthermore, nickel, molybdenum, palladium,

and ruthenium help to enhance the resistance to corrosion of unalloyed titanium in certain environmental circumstances [31, 45]. However, elements like Zr, Hf, and Sn act as neutral elements. These elements are highly soluble in alpha and beta phases, resulting in a minor decrease in transformation temperature for alpha to beta accompanied by an increase in concentrations. [44]. To create balance between the alpha and beta phases, alumina, tin, and zirconium are frequently mixed. These three elements are commonly incorporated into almost all commercial titanium alloys due to their higher solubility in the alpha and beta phases. Moreover, these elements significantly enhance the creep resistance of the alpha alloys [31].

### **2.3 Classification and grading of titanium and its alloys:**

Ti is categorized primarily on the basis of oxygen and iron concentration. Pure Titanium has less strength, hardness, and transformation temperature but generally has better formability due to lower interstitial content. The four distinct classifications of titanium alloys include alpha, near alpha, alpha+beta, and beta alloys. The alpha-beta alloy Ti-6Al-4V, which accounts for roughly 45% of all titanium production, is the most popular of them. About 30% of the manufacturing is made up of grades of pure titanium, while the remaining 25% is made up of different alloy types. The most used titanium alloys are Ti-6Al-4V and its Extra-Low Interstitial (ELI) variant (Ti-6Al-4V ELI) and (CP-Ti) grade. However, utilization of beta type alloys in implant applications has become more popular over the past ten years. Table 1 provides the relevant ASTM standards for the alloys of titanium employed in medical applications [44].

**Table 1.** In medical implants, mostly used titanium and titanium alloys according to ASTM standards.

Microstructure	ASTM standard	Alloys
$(\alpha)$	F67	Cp-Ti grade 1
		Cp-Ti grade 2
		Cp-Ti grade 3
		Cp-Ti grade 4
$(\alpha + \beta)$	F136	Ti-6Al-4V ELI
	F1472	Ti-6Al-4V
	F1295	Ti-6Al-7Nb
	F2146	Ti-3Al-2.5V
$(\beta)$	F1713	Ti-13Nb-13Zr
	F1813	Ti-12Mo-6Zr-2Fe
	F2066	Ti-15Mo

### 2.3.1 Biocompatibility of alloying elements:

A number of Alloying elements are used in fabrication of titanium alloys. Notably, Table 1 shows that the alloying elements V, Al, Nb, Zr, Mo, Fe, and Ta are crucial in implant applications. In the subsequent section, a brief summary of the toxicity concerns linked to Ti, V, and Al is presented.

#### 2.3.1.1 Titanium.

Titanium, despite its absence in summary and lack of any known biological function [45], is considered non-toxic, even in significant quantities. Studies have shown that when humans were exposed to daily doses of up to 0.8 mg of titanium, the majority of it was excreted without digestion or absorption [46]. Titanium implants generally exhibit good compatibility with the host bone, without being rejected by the body [47, 48]. Moreover, it has been observed that titanium particles exhibit size-dependent physiological impacts on leukocytes in vivo. [49, 50].

### **2.3.1.2 Vanadium:**

Vanadium's specific biological role in the human body is still not well understood [51, 52]. It has also been demonstrated to trigger both positive and negative cellular responses. [50]. Compounds of Vanadium oxides primarily cause toxicity [53]. Vanadium and its byproducts can cause carcinogenicity and a number of harmful consequences on the liver, nervous system, and other organs when either orally or inhaled, according to animal studies. [54,55]. Comprehensive research on the toxic nature of vanadium and observed a link between vanadium release and failure of implants [56].

### **2.3.1.3 Aluminum:**

The precise role of aluminum in the human body remains largely unclear despite of being natural occurrence. Aluminum is toxic in large quantities, with acute toxicity occurring at high levels. The possible consequences of chronic aluminum toxicity and its probable connections to neurological issues, however, have given rise to an increase in public concerns. [57].

Aluminum has been linked to a number of disorders and health problems. Elevated consumption of dietary aluminum may potentially hinder skeletal mineralization, leading to reduced bone density in infants due to its competition with calcium absorption. It has also been linked to blood-brain barrier issues and neurotoxic effects on the brain. Individuals with kidney disease are particularly vulnerable to aluminum toxicity, similar to other metals. Symptoms of aluminum intolerance can include contact dermatitis and digestive disorders. Furthermore, in vitro studies reveal that aluminum has the ability to adhere to estrogen receptors, resulting in higher expression of genes in human breast cancer cells.

## **2.5 Biocompatibility of titanium alloys:**

Titanium alloys have been shown to have a greater level of biocompatibility due to their remarkable corrosion resistance. [58,59]. In vitro studies indicate the usage of titanium alloys is not harmful for both human and animal subjects in terms of mutagenicity investigations. [59]. Ti-6Al-4V (Ti64), a first-generation titanium alloy, has been mentioned as having the potential of toxicity and promotes allergic reactions in the body [60]. Second-generation titanium alloys have drawn considerable attention,

with a special emphasis on beta-titanium alloys. These alloys contain beta stabilizing elements Mo, Ta, and Zr, which are reasonably safe when compared to vanadium and aluminum, as alloying elements. [61].

## **2.6 $\alpha$ titanium alloys**

The yield strength and tensile strength of alpha Ti alloys, are significantly influenced by the precise alloy compositions while young modulus remains unaffected, as shown in Table 2. By adding interstitial elements in the different concentrations, in commercially pure (CP) Ti (99.6%), composed of  $\alpha$ -titanium phase yield strength and tensile strength can vary between 240 and 550 MPa and 170 to 480 MPa, respectively. Grades of CP-Ti contain oxygen and iron, and as their content increases, the strength of the alloy also increases. Moreover, higher levels of oxygen in the alloy contribute to increased fatigue strengths. With the inclusion of beta stabilizers in low concentration, super-alpha or near-alpha alloys are categorized as alpha-alloys. Despite the presence of beta phases, they are more likely CP-Ti (commercially pure titanium) alloys. However, by having comparatively lower strength these alloys are significantly used as implants in comparison to  $\alpha$ -beta or  $\beta$  alloys. But few grades of CP-Ti are favorable in low loading applications that require relatively high corrosion resistance.

## **2.7 $\alpha$ - $\beta$ titanium alloys:**

Strength in Alpha+beta alloys can be tailored by using a combined approach that combines solution treatment and ageing operations when compared to Cp-Ti. The final microstructure of these alloys is primarily influenced by factors such as alloy composition, solution treatment temperature and solidification rate. Additionally, the modifications in the microstructure can be done through subsequent aging treatments typically conducted at 480 to 650 °C temperatures ranges. As a result of ageing, the alpha phase precipitates and a delicate mixture of alpha and beta microstructures is formed [62]. Solution and aging treatments significantly increase 30-50%, strength of alpha-beta alloys with little impact on their Young's moduli (as indicated in Table 2). Moreover, solution treatment and aging boost the fatigue strengths of these alloys greater than that of alpha alloys. The application of solution-treated and precipitation-hardened titanium alloys in production is still limited, despite extensive study on alpha-beta alloys precipitation hardening. Table 1 showed a list of four alpha-beta

alloys that are standardized by ASTM and used in medical equipment. Widely adopted standardized titanium alloys are Ti-6Al-4V and Ti-6Al-7Nb. Moreover, Ti-6Al-7Nb and Ti-5Al-2.5Fe have the same metallurgical properties as Ti-6Al-4V but they are free of vanadium. It is worth noting that toxic properties of vanadium can lead to adverse effects on tissues has been reported [31].

**Table 2** The important mechanical properties of Ti alloys based on microstructure

[31].

Materials & microstructure	Total Elongation (%)	Elastic modulus (GPa)	Ultimate tensile strength (MPa)	Yield strength (MPa)
<b><math>\alpha</math> phase</b>				
(ASTM grade 1)	24	115	240	170
(ASTM grade 2)	20	115	340	280
(ASTM grade 3)	18	115	450	380
(ASTM grade 4)	15	115	550	480
<b><math>\alpha+\beta</math> phase</b>				
(Ti-6Al-4V)	10-15	110	390	860
(Ti-6Al-7Nb)	10	105	860	795
(Ti-5Al-2.5Fe)	6	110	900	820
(Ti-3Al-2.5V)	15	100	690	585
<b><math>\beta</math> phase</b>				
(Ti-13Nb-13Zr)	10-16	79-84	970-1040	840-910
(Ti-12Mo-6Zr-2Fe)	18-22	74-85	1060-1100	1000-1060
(Ti-15Mo)	22	78	800	655
(Ti-15Mo-5Zr-3Al)	17-20	75-88	880-980	870-970
(Ti-15Mo-2.8Nb-0.2Si-0.26O)		83		950-990
(Ti-16Nb-10Hf)		81		730-740
(Ti-(10-80) Nb)		65-93		760-930
(Ti-35.5Nb-7.3Nb-5.7Zr)		55-66		800
(Ti-(70-80) Ta)		80-100		350-600
(Ti-Ta-Nb/Nb/Sn)		40-100		400-900
(Ti-Zr-Nb-Ta)		46-58		
<b>Stainless steel and Cobalt alloy</b>				
(316L)		200		200-700
(Co-alloy)		240		500-1500

## 2.8 $\beta$ titanium alloys:

Beta phase BCC titanium alloys are commonly known as "second generation titanium biomaterials". The innovation in beta alloys were motivated by a variety of issues, with one of the main objectives was to solve the problem of stress shielding induced by the higher Young's moduli of implants. Titanium alloys exhibit moduli that are generally more comparable to bone (as indicated in Table 2) [60, 61, 63-65].

By employing solution treatment followed by fast cooling rates, transition of beta ( $\beta$ ) phase to alpha phase can be prevented in beta alloys. After solution-treatment these alloys demonstrate high hardenability, remarkable forgeability combined with cold formability. Aging in temperatures ranges from 450 to 650 °C, alpha ( $\alpha$ ) phase precipitates out and disperses within the beta matrix, resulting in an optimal microstructure for precipitation strengthening [62].

Beta alloys also possess notable characteristics of being low modulus and excellent corrosion resistive materials [65], [66]. Widely employed materials in the medical field are commercially pure titanium (cpTi), as well as earlier variations of (Ti-6Al-4V) alloy. But having the potential of allergic reactions due to vanadium ions released in body [67, 68] and neurological issues linked to aluminum [70] led to the manufacturing of alternative alloys. The emergence of Ti-Nb-Ta-Zr based, Ti-Zr-based, and Ti-Sn-based alloys, aimed at addressing these concerns and ensuring biocompatibility [26, 69, 71]

In recent times, a novel group of  $\beta$ -type biocompatible alloys have been formulated and represented in Table 3:

**Table 3** Various Beta titanium systems

Binary system	Ternary system	Quaternary systems
(Ti-Nb ) [72], (Ti-Mo) [73],[74], (Ti-Ta ) [75], (Ti-Zr ) [76], (Ti-Mn ) [77], (Ti-Cr) [78], [79];	(Ti-Nb-Mo ) [80], (Ti-Nb-Pd ) [81], (Ti-Nb-Zr ) [82]-[83], (Ti-Nb-Sn ) [84], (Ti-Nb-Ta ) [85], [86], (Ti-Nb-Fe) [87], (Ti-Mo-Zr) [88], (Ti-Mo-Nb) [89], (Ti-Cr-Al) [90], [91], (Ti-Cr-Nb) [92], (Ti-Cr-Sn) [93], (Ti-Mn-Al) [94], (Ti-Ta-Nb system) [95], (Ti-Ta-Sn system) (Ti-Ta-Zr system) [96], (Ti-Mn-Fe) [97], (Ti-Sn-Cr) [58];	(Ti-Ta-Sn-Zr) [98], (Ti-Nb-Zr-Sn) [99], [100], (Ti-Nb-Zr-Fe) [101], (Ti-Nb-Ta-Zr) [102]- [103-105], (Ti-Mo-Zr-Fe) [106], (Ti- Fe-Ta-Zr) [107], (Ti-Cr-Mn-Sn) [108],

## 2.9 Research gap:

A valuable physical characteristic of implant materials is their elastic modulus, especially in loading conditions. It plays a significant role in preventing the "stress shielding effect,". It is required to minimize the mismatch of elastic modulus between implant material and the surrounding bone to ensure proper integration and long-term stability [60, 61].

In general, metallic implants have a higher elastic modulus than bones, and they also have stress-strain characteristics that do not resemble the plateau-shaped behavior that is typical for bones. The Young's modulus should closely resemble those of bones when considering the choice of materials to replace bones that have been worn down or damaged. Binding forces and crystal structure are the factors that affect the young modulus of the materials. Consequently, there has been a concerted effort in recent



years to conduct extensive research and make significant advancements to improve this property of Ti alloys, in achieving lower values of (E) elastic modulus [63, 64, 65].

### **2.9.1 Efforts to reduce elastic modulus:**

Different approaches have been employed in literature to control the elastic modulus and lower its value to meet the bone requirements.

#### **2.9.1.1 Alloying.**

A favorable choice in orthopedic applications over other implant materials is Ti alloys due to several advantages they offer. These include their comparatively lower stiffness, excellent cytocompatibility, high resistance to corrosion, and favorable strength-to-modulus ratio. The variety and composition of alloying materials as well as the particular processing techniques used are among the factors that can change the microstructural features that have an impact on the elastic modulus of Ti alloys. Beta phase exhibits elastic modulus lower when it is compared to the hexagonal phase. As a result, researchers have developed and continue to develop several  $\beta$ -type titanium alloys that primarily consist of elements known for their low toxicity and lack of allergenic properties, particularly the elements mentioned earlier. These alloys are specifically designed to have lower Young's moduli and are suitable for biomedical field given in Table 4 [130].

**Table 4.** Elastic modulus of various Beta type alloys

<b>Alloy</b>	<b>Elastic modulus (Gpa)</b>
(Ti7.5Mo3Fe)	85
(Ti15Mo2.8Nb3Al)	82
(Ti15Mo)	78
(Ti13Nb13Zr)	77
(Ti12Mo6Zr2Fe)	74-85
(Ti29Nb13Ta6Sn)	74
(Ti29Nb13Ta4Mo)	74
(Ti12Mo5Ta)	74
(TLM Alloy)	67
(Ti35Nb5Ta7Zr0.40)	66
(Ti29Nb13Ta4.6Sn)	66
(Ti25Nb2Mo4Sn)	65
(Ti29Nb13Ta4.5Zr)	65
(Ti-12Mo5Zr)	64
(Ti29Nb13Ta2Sn)	62
(Ti29Nb11Ta5Zr)	60
(Ti28Nb13Zr0.5Fe)	58
(Ti35Nb5.7Ta7.2Zr)	57
(Ti35Nb7Zr5Ta )	55

**2.9.1.2 Heat treatment and thermo mechanical processing:**

Thermo-mechanical processing (TMP) plays a vital role in reduction of stiffness in  $\beta$  phase alloys. According to Bertrand et al. [109], they successfully lower elastic modulus to 55 Gpa of a Ti-25Ta-25Nb alloy. The significant reduction was attained through a specific TMP technique that involved cold rolling with an 80% reduction, followed water quenching after solution treatment for half hour at 850C°. This

treatment restored a fully recrystallized microstructure in the  $\beta$  phase, resulting in a reduced grain size and ultimately lowering the elastic modulus.

Heat treatment is a commonly employed process to effectively control young's modulus of titanium alloys. In some cases, solution treatment can result in a favorable matching of elastic moduli due to the formation of specific phases, as explained by Changli Zhao et al. [110], they investigated a Ti-12Mo-5Zr alloy that exhibited a structure consisting of acicular martensitic phases along with the beta phase. After undergoing solution treatment, the alloy showed elastic modulus 64 Gpa, which contributed to improved mechanical biocompatibility.

### **2.9.1.3 Introduction of porosity:**

In an effort to address the issue of stress shielding in implants associated with bulk materials, porous structures have been introduced. Modifying the elastic modulus of bulk materials is a difficult task, as it is an inherent property. However, by utilizing porous materials, the available material for a given cross section is reduced, thereby leading to a reduction in elastic modulus. Considerable research efforts have been made to comprehend the essential features and properties for the effective utilization of porous materials. Mechanical properties porous Ti-based alloys are directly related to various factors, level of porosity, morphology of pore, size distribution of pores, and microstructure. Porosity evaluates the macroscopic mechanical properties of materials. Deformation behavior of pores in compression is different for alloys which have higher plasticity than the brittle ones. The pore size and amount of porosity also beneficial to promote the growth of tissues [111-114].

In a study, 78% of porous titanium foams fabricated by Wen et al. [115] exhibited a compression strength and modulus of elasticity i.e., 35 MPa and 5.3 Gpa respectively. In a different study [116] for Ti-Zr alloy foams with 70% porosity, compressive plateau strength of 78.4 MPa, and elastic modulus of 15.3 Gpa was found. In a study conducted by Wang et al. [117] created a Ti-10Nb-10Zr porous alloy containing 69% porosity level, the foam had a elastic modulus of 3.9 Gpa and a 67 MPa compressive plateau.

The fabrication of porous metallic structures can be produced using several techniques, including as space holders, gas injection, blowing agents, dynamic freeze casting, and additive manufacturing [119-125]. The gas injection technique involves injecting

pressurized gas into the liquid material, which forms tiny bubbles that, as the substance cools, solidify into a porous structure. Controlling the viscosity, which can be done by adding ingredients like Al<sub>2</sub>O<sub>3</sub>, SiC, and MgO, is essential for this process. This method, however, is not appropriate for substances that are readily oxidized. Adding a blowing agent to the melt causes it to release gases when heated, which is how the blowing agent technique works. If the blowing agent gets stuck in the material, the challenge in this process is getting it out [122]. Porous structures can also be created using deep freezing techniques, although because of the high oxygen content, the resulting structures may be weak [125]. Porosity can be precisely controlled by additive manufacturing, which includes powder bed fusion and direct energy deposition methods [119, 125], however it can be expensive. Control over porosity and pore size is quite good with the space holder method. Metallic powders are mixed with substances that help hold space, such as ammonium carbonate, carbamide, dolomite, and titanium hydride. A porous construction is left behind after heating to the point where the space-holding material melts. It can be difficult to choose a holding substance that is appropriate for the space and to make sure it is completely removed. Furthermore, all combining components must be in powder form when using the space holder approach.

## **2.10 Our chosen alloy:**

The quest for an alloy that possesses desirable features while absence of dangerous elements is of enormous significance. The problem of toxic elements has been a matter of great significance.

Previous research has indicated that alloys comprising (Nb), (Ta), and (Zr) elements have better biocompatibility because they are toxic free elements [126]. In comparison to the metal and alloy implants now in use, the alloy Ti-35Nb-7Zr-5Ta exhibits a lower Young's modulus of 55 Gpa, which is relatively low towards the modulus bone [5]. In titanium alloys Zr behaves as neutral element and form solid solution in Beta and alpha phases. When added in low amounts, the malleable and ductile metal niobium (Nb) considerably improves the alloy's mechanical properties. Additionally, Nb stabilizes the Beta phase and can lower the elasticity modulus [127]. A titanium alloy containing Nb is a good option for implant applications because of these properties. Tantalum (Ta) addition in the alloys helps in reducing the elastic modulus, when alloyed with

commercially pure titanium, bringing it closer to the elastic modulus of bone [119, 128].

# Chapter:3

## Experimental Techniques

This chapter includes detailed descriptions of the experimental and characterization methods utilized for the sample production and analysis. Thermocalc software and the Tchea database were used for developing multiple alloys, and their corresponding alloy buttons were made in a vacuum arc melting furnace using argon as the environment. The following steps are involved in the design and development of alloys and their corresponding foams:

### 3.1 Alloy preparation:

To develop alloy buttons, arc melting of a pure mixture of Ti (99.95%), Nb (99.95%), Ta (99.95%), Zr (99.95%), and Y (99.95%) was done in an environment of titanium getttered argon. A copper hearth that is water cooled and has five crucibles is inside the furnace chamber. At 10-5 torr, the vacuum inside the chamber is maintained. Figure (5) depicts the schematic for the vacuum arc melting furnace in use.

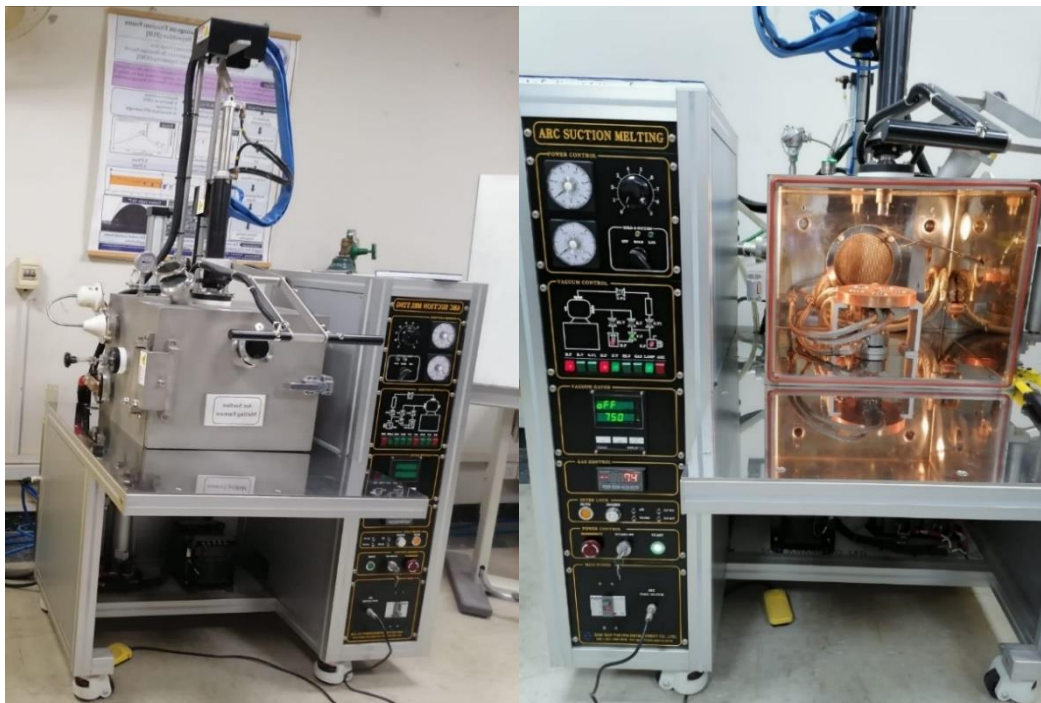


**Figure 5** Vacuum arc melting furnace.

The titanium getter placed in the hearth crucible is heated to melt, removing the oxygen from the chamber before melting the raw components. When a significant

value of current flows through a tungsten electrode, an arc is produced that causes melting to occur. The alloy melt was turned upside down and melted again after the initial cycle. Five rounds of this melting process are required to ensure the homogenization of the alloying element. The metallic alloy buttons, as depicted in Fig. 6, are then taken out of the furnace and sliced into samples with the required dimensions using EDM wire cutting.



**Figure 6.** Solidified alloy button

### **3.2 Grinding and polishing:**

In order to prepare samples for electrochemical tests, microstructure characterization, crystal structure and phase identification, alloy buttons are wire-cut using EDM. After this, samples are mounted in bakelite powder using a hot mounting press at 180°C for microstructural analysis (fig.7).



**Figure 7** Mounting Machine and mount.

The next step is the following grinding and polishing the mounted samples. Silicon carbide emery papers with grit sizes ranging from P600 to P2000 are used for grinding. In order to achieve a scratch-free surface, the mounted samples were polished using alumina slurry of 1 and 0.5. Fig. 6 depicts a grinding and polishing machine used to prepare samples. After grinding and polishing, samples were sonicated for five minutes each in ethanol and deionized water to remove alumina particles from the surface. Microstructural characterization and electrochemical tests are then performed on the prepared samples.



**Figure 8.** Polishing Machine.

### **3.3 Dealloying:**

Dealloying is the process of retaining the more stable phases and components of the alloy while removing the less stable ones. The goal of the current work was to remove the filler metal from the interdendritic region, creating a foam-like structure with interconnected 3D porosity. The samples' weights were calibrated before dealloying. For around 24 hours, samples were individually dipped in a solution of  $\text{HNO}_3$ +HF in deionized water. The samples were then carefully cleaned for five minutes each with ethanol and deionized water. After sonication, they are heated to  $130^\circ\text{C}$  and dried on a hot plate for 15 minutes. After drying, the samples are weighed once more to determine the % weight reduction. To compare the microstructural and phase changes before and after dealloying, de-alloyed samples were then characterized using SEM and XRD.



### **3.4 Characterization of samples:**

#### **3.4.1 SEM:**

To analyze the microstructure of Ti-35Nb-5Ta-7Zr, SEM analysis of the as cast sand de-alloyed samples was conducted. SEM is a powerful imaging method used to obtain high-resolution, three-dimensional images of samples at the micro- and nanoscale. SEM works by interacting electrons with the sample surface. Here's how the SEM works:

- i. SEM uses an electron source, often a heated filament or a field emission source, to generate a beam of high-energy electrons. To accelerate a high voltage is applied.
- ii. The accelerated electron beam passes through a number of electromagnetic lenses, which concentrate and shape the beam into a small, tightly focused point.
- iii. The sample for SEM analysis must be properly prepared. To increase image quality and reduce charging effects, it is often coated with conductive material, i.e., gold or carbon.
- iv. The concentrated electron beam is then raster-scanned across the sample's surface. Various processes occur when electrons from the beam contact the sample, including Secondary Electron. High-energy electrons from the primary beam are capable of knocking secondary electrons off the sample's surface. Secondary electrons contain information about the surface topography, composition, and material contrast of the sample. Because of interactions with atomic nuclei, some primary electrons are scattered back from the sample surface. Backscattered electrons reveal information about the sample's atomic number and composition. When high-energy electrons encounter the atoms in the sample, they can emit distinctive X-rays and determine chemical composition.
- v. Secondary electrons, backscattered electrons, and X-rays are collected by detectors located above or below the material. These signals are amplified and processed after having been converted to electrical signals.

- vi. A detailed image is created by raster scanning the electron beam across the sample surface and measuring the emitted signals. To visualize the topography, composition, and other features of the sample, the intensity of the signals is transformed into grayscale or color representations.

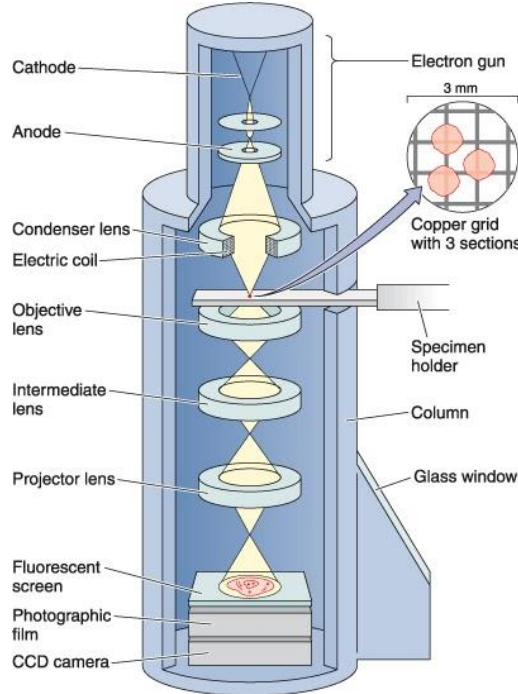


**Figure 9.** Working principle of SEM.

Fig. 9 depicts the SEM's mechanism. Scanning electron microscope (JEOL-JSM6490LA) with an EDX detector, NUST as shown in Fig. 10, was used to determine the chemical composition and morphology of as-cast and de-alloyed samples.

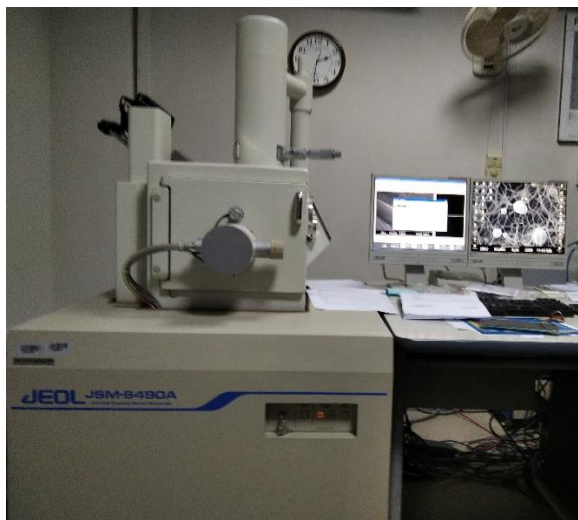


**Figure 10.** Scanning electron microscope setup.

### 3.4.2 X-ray diffraction (XRD):

A non-destructive method for examining the crystal structure and identifying material phases is X-ray diffraction. The cathode ray tube's filament is heated that produce electrons and they get accelerated in the direction of the specimen by providing voltage, according to the x-ray diffraction's working principle, which involves the constructive interference between incident rays and satisfies Bragg's Law, which is given as:

$$n = 2d \sin$$

These electrons strike the specimen surface with enough energy to knock off the inner shell electrons, which causes the emission of distinctive x-rays. When Bragg's Law is met by the incident rays, constructive interferences take place. It ends up in the emergence of an intensity peak. Schematic of x-ray diffraction is shown in Fig. 9.

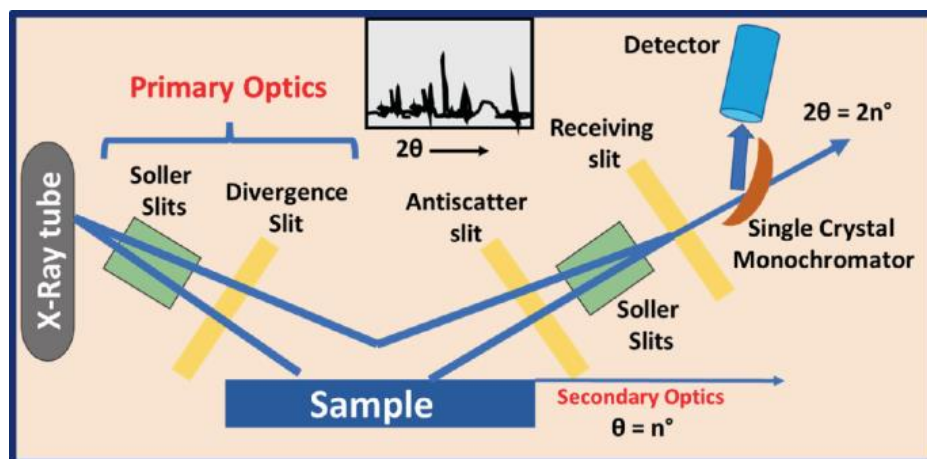


**Figure 11.** XRD working principle.

For the XRD analysis, 1mm thick EDM wire cutting samples were used. The samples were thoroughly sonicated in ethanol and then in deionized water before being put through to additional grinding to level the specimen surface.



**Figure 12.** XRD equipment at SCME NUST.

### **3.5 Mechanical testing:**

#### **3.5.1 Compression:**

To determine the material's response to compressive loadings, the specimens were undergoing compression testing. We can assess several mechanical properties with the aid of compression tests, including yield strength, young modulus, elastic limit, and compressive strength, which are crucial to determining whether the systems we create have the desired features for the applications we want them for, or if new systems need to be developed for those applications. Because the ingot we produced in the furnace is too small to prepare a sample for a tensile test, we do compression testing. In order to cut the button-shaped alloy created from the arc suction melting furnace, we used EDM wire that was cut into the required geometry in accordance with ASTM standard E9. Fig. 13 displays the sample under compression testing.



**Figure 13.** Alloy sample During compression testing

The universal testing machine (UTM) SHIMADZU used to conduct compression testing shown in Fig. The strain rate on the UTM was set at  $1 \times 10^{-4}$  seconds, as documented in the literature. However, the biggest issue that arises during compression testing of such thin specimens is referred to as buckling effect, which is defined as "unstable lateral deformation of test specimen" and occurs when the specimen's mating surfaces are not exactly flat. To ensure that the sample's surfaces are completely flat, we prepare it by grinding to provide an even distribution of force along the cross-section surfaces.

The elastic modulus and yield stress values were determined by taking an average of the findings from three samples of each composition that were manufactured and tested.



**Figure 14.** Universal testing machine at SCME NUST

### **3.5.2 Microhardness:**

To assess the hardness or resistance to penetration of small or thin materials, micro hardness tests were performed. Hardness testing was done on polished mounted samples and after that measured the hardness of materials using a pyramid-shaped diamond indenter, and it caters to both micro and macro scales. When a load of up to 1000g is applied to the indenter the surface of the material is deformed plastically. The indenter's shape determines the indentation's shape. Vickers tests require precise measurement of the indent on the material's surface. The hardness of materials is then determined using these values by using formula. Ti-35Nb-5Ta-7Zr foams used in the

study had their microhardness evaluated by applying a 100gf load while the dwell time for indentation was 15sec. Cell wall indentations were made to determine the microhardness of foams. Each sample had a minimum of 12 indents created in order to calculate the average. Vickers' hardness of porous samples was measured using identical parameters for comparison.



**Figure 15.** Micro Vickers hardness testing machine

### **3.6 Wetting angle testing:**

The contact angle measurement is essential to implant design as it provides insightful information about samples' hydrophobic or hydrophilic nature. A more hydrophilic implant material is ideal because it promotes bone ingrowth and blood flow through the porous structure, lowering the risk of aseptic loosening or implant failure. A drop shape analyzer (DSA 25, KRUSS) measured the contact angle by dropping a drop of water on the surface of samples. Based on this investigation, the contact angle was measured, and the wettability was determined.

### **3.7 Electrochemical testing:**

The produced foams were subjected to electrochemical characterization, and the results were evaluated. On the Gamry workstation in SCME, NUST, corrosion

experiments were conducted. Corrosion experiments were conducted using a three-electrode arrangement shown in fig 16. Working electrode is a test specimen with a  $0.56 \text{ cm}^2$  exposed surface area. The counter electrode was platinum wire, while the

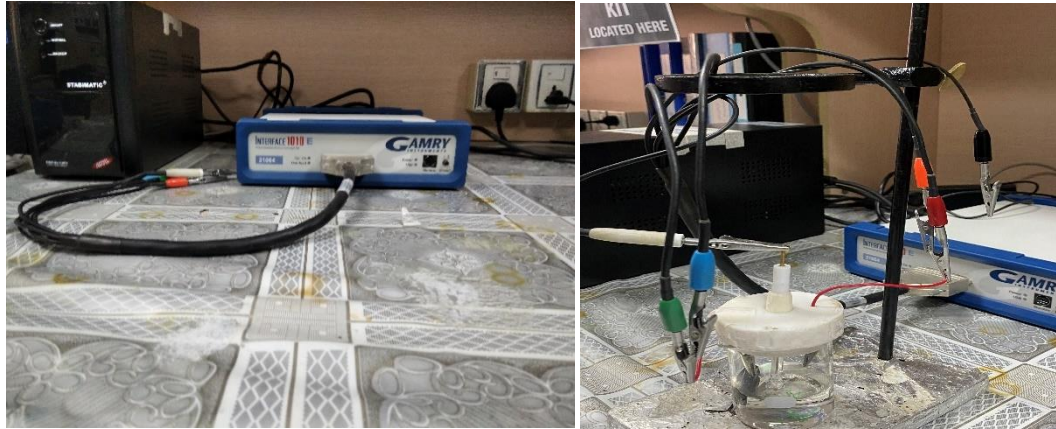


**Figure 16.** Gamry workstation for electrochemical testing.

reference electrode is Ag/AgCl.

Corrosion experiments were conducted in hank's solution  $370^\circ\text{C}$  with an electrolyte having a pH of 7.4. OCP measurements were made for 3600 seconds. Between 100000Hz and 0.01Hz, electrochemical impedance spectroscopy test was carried out. The equivalent circuit was created using Gamry software and developed in accordance with the system. Impedance data was then examined after being fitted with the created equivalent circuit. Additionally, samples were polarized in the anodic direction at a scan rate of  $2\text{mV/s}$  from  $-1500\text{mV}_{\text{ocp}}$  to  $3000\text{mV}_{\text{ocp}}$ .

### **3.7.1 OCP:**

The difference in potential between two electrodes in an electrochemical cell or system when no current flowing is referred to as the open circuit potential (OCP). It is the voltage that forms between the two electrodes when they are linked to one another, but the cell is not connected to a load or external circuit to it.

The open circuit potential, a fundamental characteristic of an electrochemical system, is influenced by the chemistry of the electrolyte and the thermodynamic characteristics of the electrode materials. With a high-impedance voltmeter or potentiostat, the voltage can be measured without any current flowing, which allows the estimation of the OCP. The open circuit potential can reveal essential information about a system's

electrochemical behavior, including the value and direction of the electrochemical potential forces that drive the reactions at the electrodes, the kinetics of those reactions, and the stability of the working electrode in the electrolyte.

### **3.7. 2 EIS:**

EIS is an electrochemical experimental technique for examining the electrochemical characteristics of materials and systems. In EIS, AC voltage is applied, and response of current is measured at various frequencies. The impedance, an intricate number that contains both magnitude and phase information, is the system's frequency-dependent response. Numerous electrochemical parameters, including resistance, capacitance, and reaction kinetics, can be identified by examining the impedance spectra generated from EIS experiments. In many disciplines, including electrochemistry, corrosion science, and materials science, EIS is extensively used. It is a non-destructive technology that can reveal details on the interactions and behavior of electrodes in electrolyte. In addition to studying the characteristics of coatings and thin films on metals, EIS can be used to characterize the efficiency of batteries, fuel cells, and other power conversion technologies. EIS is a useful tool for understanding the electrochemical behavior of materials and systems and for enhancing their performance in a variety of applications.



# Chapter:4

## Results and discussion:

The objective of this research work was to create porous structure in Ti-35Nb-5Ta-7Zr alloy, addressing the issue of the stress shielding effect by achieving a low elastic modulus. Characterization techniques, (XRD), (SEM), and energy-dispersive X-ray spectroscopy (EDS) were done to analyze development of porous structure. Compression testing was done and the mechanical behavior of developed porous alloys were evaluated, specifically elastic modulus.

The corrosion of the implants in body fluids was another significant issue that needed to be addressed in this investigation. Corrosion testing was done to determine the corrosion behavior of developed porous structures.

### 4.1 Development of Ti-35Nb-5Ta-7Zr porous alloy:

Alloying elements Ti, Nb, Ta, and Zr were selected for alloy preparation. These elements were prioritized because of better biocompatibility, good mechanical properties, and excellent corrosion resistance.

Proposed strategy was to Introduce porosity in the bulk alloy is the proposed strategy to present a solution regarding the issue of stress shielding in implant applications. The strategy was to add a filler element in the alloy which on solidification segregate on the interdendritic areas and the removal of filler element in the later stage selectively. For the filler element to segregate at the interdendritic areas in the solidification process it should be insoluble in the matrix. For a difference in the enthalpy of mixing of yttrium is greater with all elements involved in the Ti-35Nb-5Ta-7Zr system enabling it insoluble in the matrix. This is the reason yttrium was chosen as the filler element. Enthalpy of mixing of selected elements is provided in the Table 5.

**Table 5.** Enthalpy of mixing of elements selected for the system.

	Ti	Nb	Ta	Zr	Y
Ti	0	2	1	0	15
Nb	-	0	0	4	30
Ta	-	-	0	3	27
Zr	-	-	-	0	9
Y	-	-	-	-	0

Yttrium possesses the most positive enthalpy of mixing as shown in the table, so it can be inferred that upon solidification it will segregate in the interdendritic areas. The phase diagram of Ti-35Nb-5Ta-7Zr with Yttrium calculated through ThermoCalc software also supports this hypothesis. Selected composition for this study is represented by the dotted line the Fig. 17.

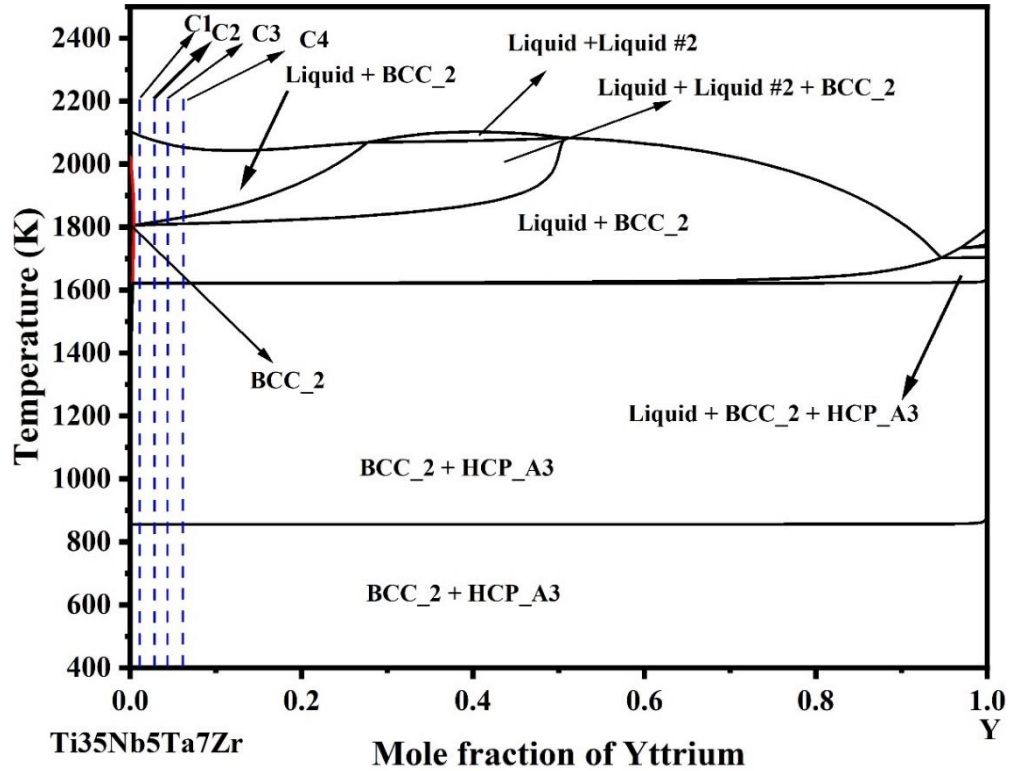
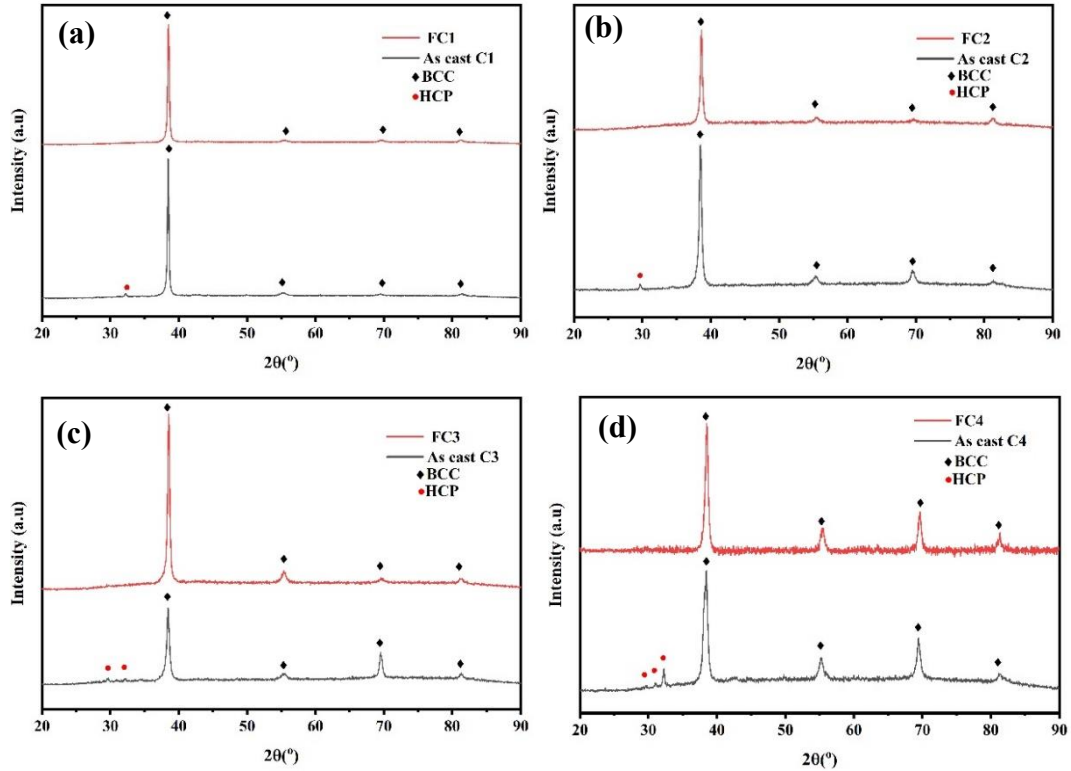


**Figure 17.** Pseudo binary phase diagram between Ti-35Nb-5Ta-7Zr and Yttrium

#### 4.2 Phase analysis:

X-ray diffraction was conducted to analyze Phase composition of the alloys under study. Ti-35Nb-5Ta-7Zr is an extensively investigated system characterized by a single beta body-centered cubic (BCC) phase composition. [129]. Inclusion of yttrium in the base alloy revealed the presence of new phase in as cast C1 to C4 alloys. Analysis of graphs showed that the newly emerged phase corresponds to Hcp phase of yttrium. From the XRD graphs it was obvious that with addition of yttrium the intensity of peaks relevant to Hcp was increased. As-cast samples were de-alloyed in

solution ( $\text{HNO}_3+\text{HF}$  and DI water) to generate porosity in the bulk structure. XRD patterns of de-alloyed samples confirmed the absence of Hcp peaks from the structure. The XRD graphs of FC1 to FC4 show that only BCC phase is present after de-alloying.



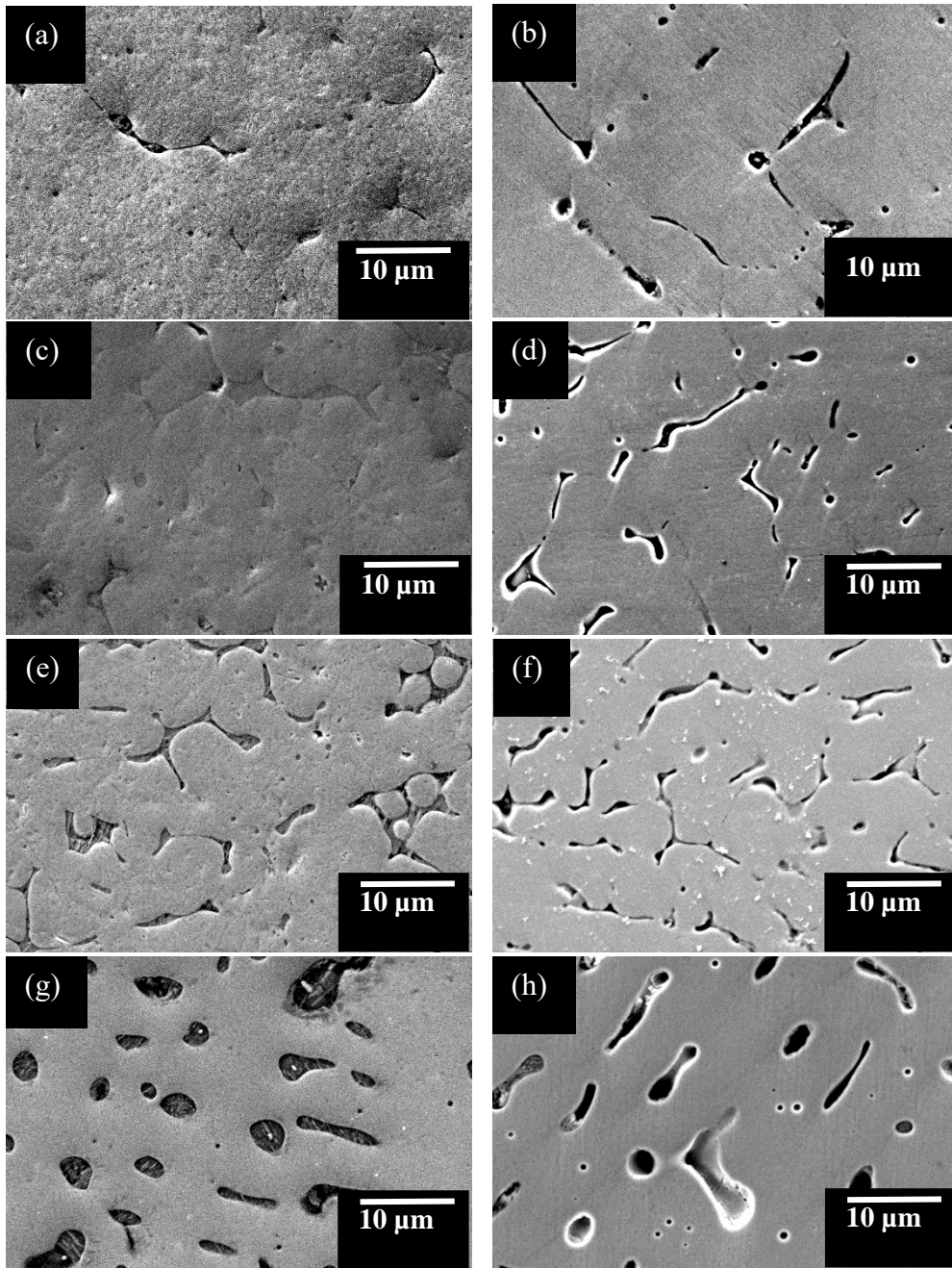
**Figure 18.** XRD pattern of (a) as-cast FC1 and de-alloyed FC1 (b) as-cast C2 and de-alloyed FC2 (c) as-cast C3 and de-alloyed FC3 (d) as-cast C4 and de-alloyed FC4

Fig. 18 illustrates the XRD graphs of as cast samples and their respective de-alloyed samples.

### 4.3 Scanning electron microscopy:

As cast and de-alloyed microstructure of the samples was investigated through scanning electron microscopy to understand the composition and analyze the effects of incorporating yttrium into the Ti-35Nb-5Ta-7Zr. Ti-35Nb-5Ta-7Zr alloy is a well explored system that is composed of single-phase BCC [129]. It was assumed that because of higher difference between enthalpy of mixing of yttrium it will segregate on interdendritic areas. Addition of yttrium in the bulk Ti-35Nb-5Ta-7Zr resulted in the segregation of yttrium in the interdendritic regions. The presence of yttrium as a filler element had also a certain impact on the size interdendritic regions. Increasing amount of yttrium, suppressed the grains size, resulting in more homogeneous and finer

structure. This observation is clear from Fig. 19 (a, c, e, g). B. Poorganji et al. stated in a study that the by adding yttrium in titanium beta alloys resulted in a refined microstructure, and even a small amount of yttrium 0.05% in the  $\beta$  alloy successfully inhibited grain growth. The transformation from single phase to dual phase with increasing amount of yttrium is evident by the XRD analysis of as-cast samples. Light grey regions in the microstructure represents matrix which is mainly comprises of Titanium, niobium, tantalum, and Zirconium where dark grey region are interdendritic areas where yttrium has segregated during solidification. Titanium, niobium, and tantalum are homogeneously distributed in the matrix, zirconium is mostly distributed in matrix but also along the grain boundaries with yttrium. Interdendritic regions are mainly enriched with yttrium along with a small amount of yttrium is present in the matrix. The elemental mapping shown in Fig. 20 determines the distribution of elements in C2 as cast sample. As interdendritic areas are highly prone to solution and have a higher affinity to react with solution than the matrix. Yttrium was selectively removed from the systems by de-alloying process. Fig. 19 (b, d, f, h) shows that after de-alloying, yttrium was selectively removed from the interdendritic regions and matrix remained unaffected. XRD analysis in Fig. 18 of the de-alloyed samples verified the presence of only one phase BCC, however the absence of HCP peaks in the graphs ascertains that yttrium has been removed from the interdendritic areas.



**Figure 19.** As cast SEM images of (a) C1, (c)C2, (e)C3, (g) C4,) and dealloyed (b)FC1 (d) FC2 (f) FC3 (h) FC4

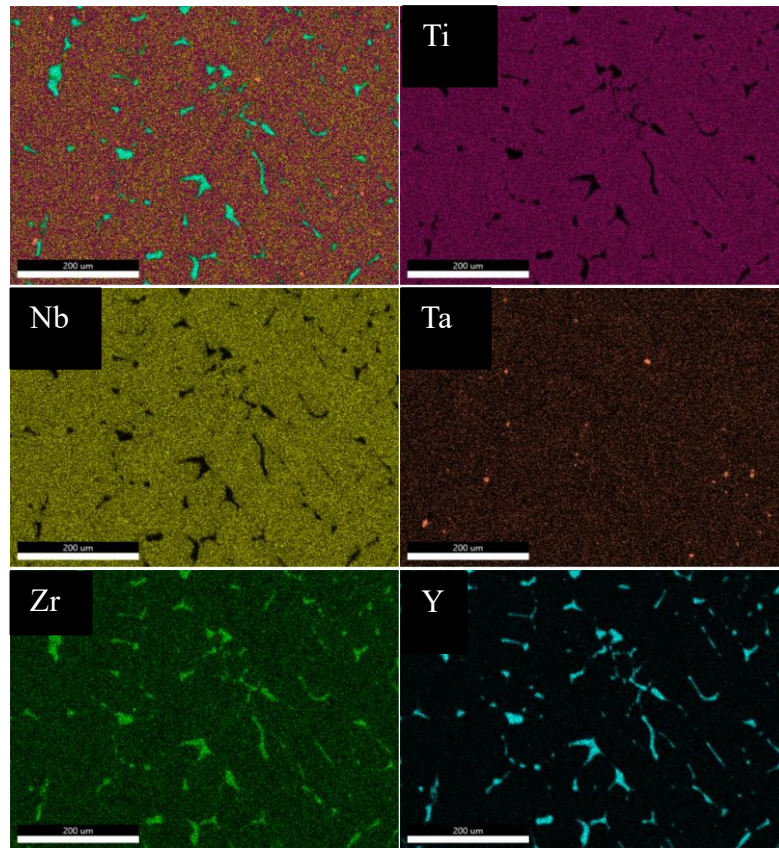


**Figure 20** EDX mapping of as cast C2.

#### **4.4 Weight loss method:**

An additional methodology based on percentage weight loss measurement was used to validate the removal of yttrium from the matrix. Weight of all samples were measured prior to chemical dealloying process to determine % weight loss. Loss was then compared to the amount of yttrium added to the composition in alloy making, to ensure that the removal was successful. In order to prepare the samples for testing, they underwent a 24-hour soaking process in a solution of HNO<sub>3</sub>, HF and DI water. The weight loss observed during the dealloying process revealed that the filler element, yttrium, had been efficiently removed from the interdendritic regions. The percentage weight loss measurement technique provides a reliable means of confirming the removal of yttrium and the successful transformation of the alloy into a foam structure. Fig. 21 shows the percentage weight loss of all developed samples.

The finding obtained from the characterization techniques SEM, XRD and weight loss method supports the formation of porosity in alloys.

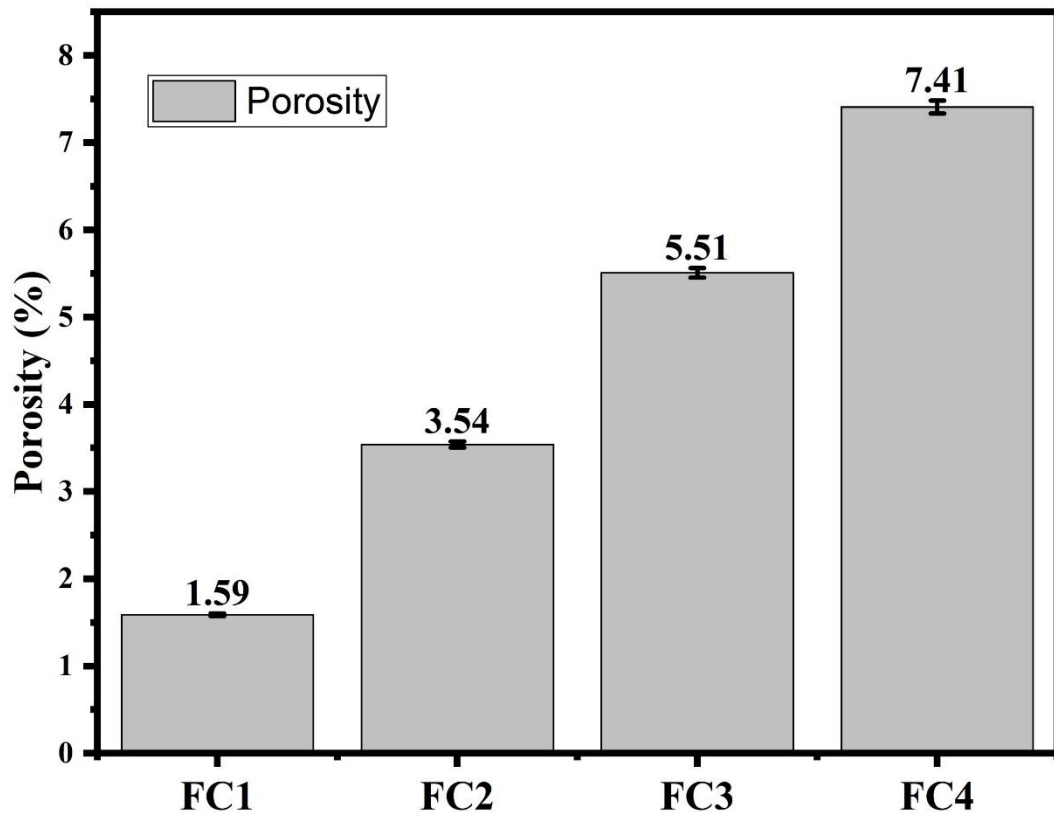


**Figure 21** Weight loss data of dealloyed samples.

#### **4.5 Mechanical properties:**

As cast Ti-35Nb-5Ta-7Zr alloy showed an elastic modulus of 55 Gpa, according to information mentioned in the literature. This alloy presents the lowest elastic modulus in Beta phase alloys with excellent biocompatibility and corrosion resistance properties [130]. But it is still higher in comparison to the bone (30 Gpa). In an effort to lower the elastic modulus close to the natural bone, different levels of porosity were induced in the Ti-35Nb-5Ta-7Zr alloy. The effect of induced porosity on the mechanical properties was evaluated by compression testing. The objective was to understand how the elastic modulus of material behaves in the presence of porosity under compression state. Stress strain curves for porous alloys are presented in Fig. 22. A decreasing trend in elastic modulus with an increase in porosity was observed. FC1 exhibits the elastic modulus of 29Gpa with almost 1.6 % porosity while FC4 presents the lowest elastic modulus of 13.7Gpa with porosity level of 7.34%. Findings of the results revealed that yield strength of the developed porous alloys decreased with the increasing level of porosity. The yield strength of FC1, FC2, FC3, and FC4

was found to be 293.98, 273.18, 258.60 and 215.12 MPa respectively. This decrease in mechanical properties is due to the reason that incorporation of porosity adds discontinuities in the microstructure cause a reduction in mechanical properties yield strength and elastic modulus.

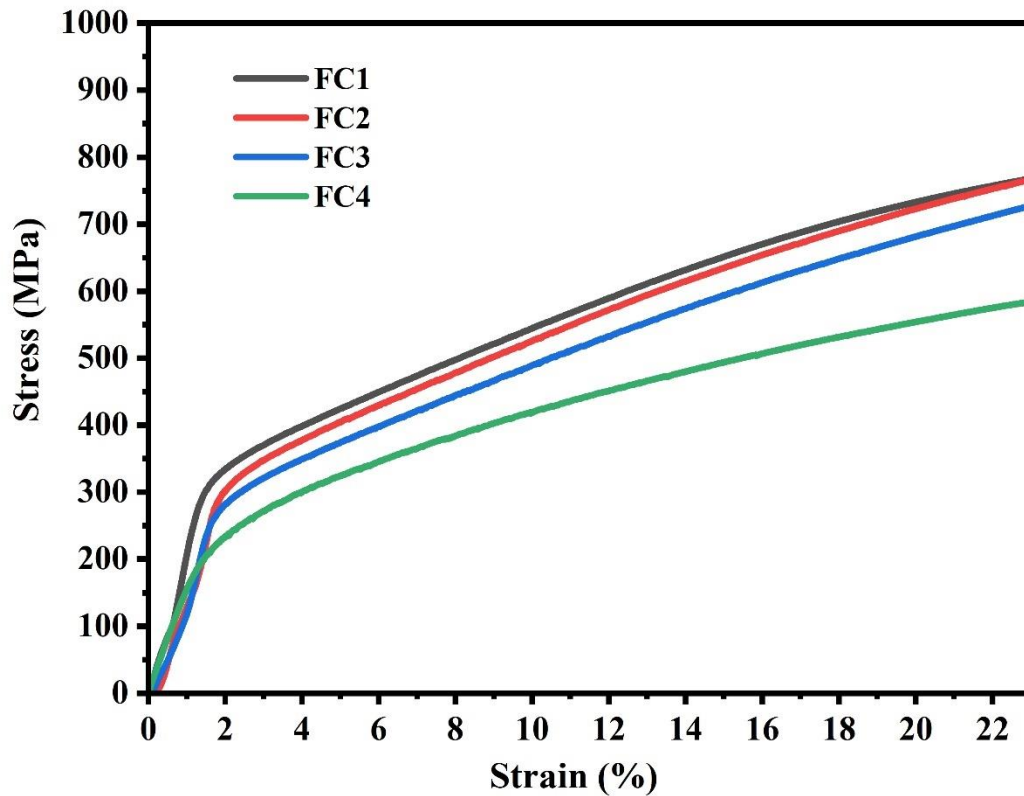


**Figure 22** Compressive stress strain graphs of Dealloyed samples FC1 to FC4

Developed porous samples showed modulus of elasticity that fall in the range of cortical bone. The modulus of elasticity of developed porous alloys as result of porosity is compared with the natural bone. Modulus of elasticity of FC1, FC2, FC3 and FC4 observed to be in the range of cortical bone (10 to 30 Gpa) Fig. 23. The findings show that these created foams have the potential to replace the cortical bone. Similar trend was observed in yield strength of the foams and compared with the natural bone. The yield strength of the foam dropped from FC1 to FC4, yet it remained higher than that of bone. This suggests that the foam can endure higher levels of stress than bone under different loading conditions. In other words, despite a small drop in yield strength among the different foam samples, the foams have greater load-bearing capabilities when compared with cortical bone.



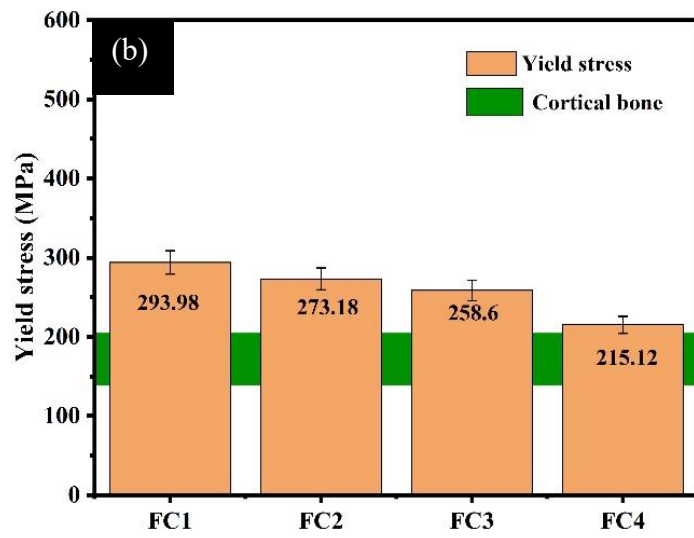
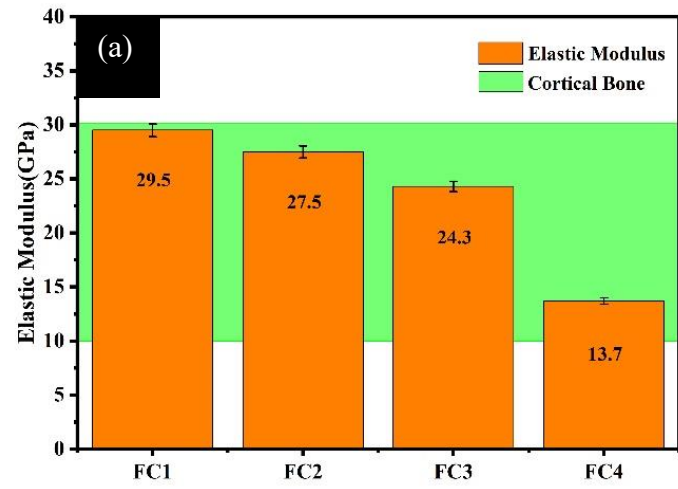


**Figure 23** Comparison of Elastic modulus of bone with (a)elastic modulus (b) Yield stress

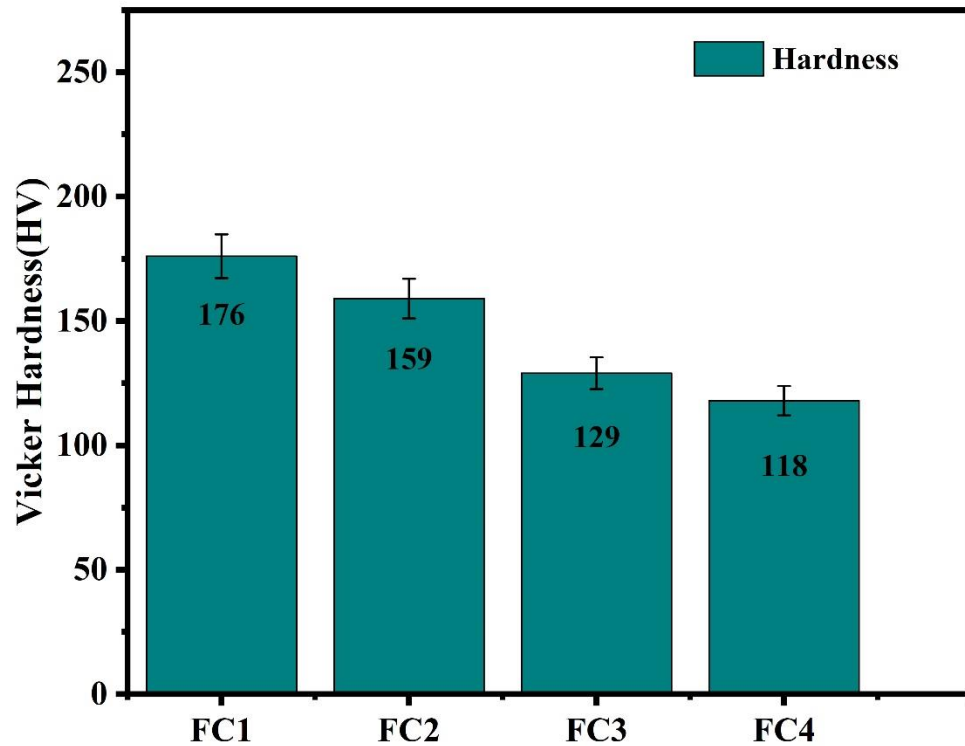


**Figure 24** Hardness of developed porous samples.

A similar trend in the hardness values was observed in the developed where an increase in porosity level decreases the hardness. The Micro-Vickers hardness of the FC1 was 176 whereas FC4 showed hardness of 118 HV. The hardness of the developed foams of Ti-35Nb-5Ta-7Zr are presented in Fig. 24. Foam fabricated in this work exhibited a higher level of hardness than the bone, indicating better resistance to indentation and deformation as the hardness of the natural bone is 47.3 HV.

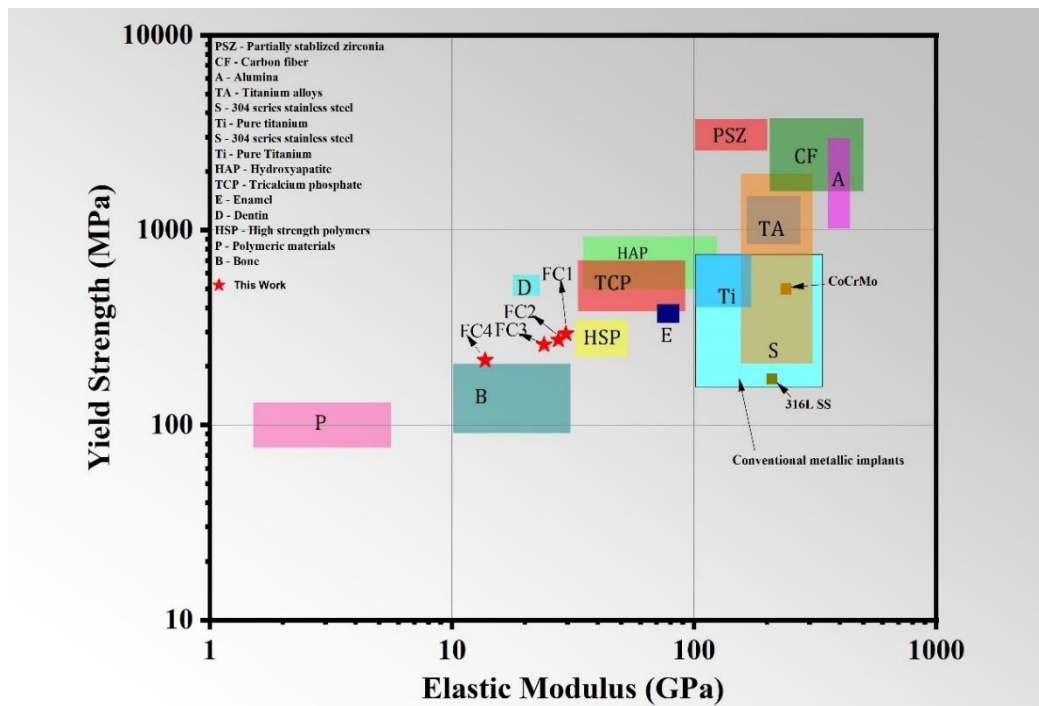


**Figure 25.** Comparison Yield strength and Elastic modulus of Developed porous alloys with literature.

Fig. 25 illustrates an Ashby-type diagram mapping elastic modulus versus yield strength of biomaterials, effectively demonstrating the unique properties of the produced Ti-35Nb-5Ta-7Zr foams. The results of this research show that there is a substantial amount of vacant space in the diagram, especially at higher values of yield strength combined with lower elastic modulus. This shows that the developed Ti-35Nb-5Ta-7Zr foams have characteristics not previously observed in non-porous and porous metallic implants. The high yield strength combined with low elastic modulus indicates that these materials have the potential for better mechanical performance while opening opportunities for biomedical applications. The mechanical properties of the developed foams were compared with those of previously mentioned biomedical implants materials, i.e., 316L stainless steel [39], CoCrMo [40], CP-Ti [41], Ti-6Al-4V [42], Ti-13Nb13Zr [43], and various other -type titanium alloys [10,44-49]. The balance of a low modulus, high yield strength with appropriate ductility is essential for the fabrication of an ideal metallic biomaterial. In comparison to other biomedical alloys that have been examined, the porous alloys fabricated in this study showed an excellent pair of high yield strength and a notably lower value of elastic modulus, which provides long-term functionality in addition to near-net shape processing abilities.

#### 4.6 Wetting angle:

Wetting qualities are the characteristics of a surface that determine how a substance interacts with liquids, particularly how the liquid spreads or beads up on the surface. The wetting characteristics of biomaterials or implants have an impact on the growth of hard tissues like bone or dental tissues. Contact angle and porosity have an inverse relationship. There is a noticeable tendency noticed as porosity increases in which liquid penetration gets deeper and the measured contact angle lowers [21,22]. High contact angle was observed for FS2 as it has the less porosity, FS5 showed the least contact angle among all the samples as it contains higher porosity. The contact angle results are consistently less than 90 degrees across all samples. Even though the materials under evaluation have polished surfaces, this shows that all the samples have a relatively hydrophilic nature. Contact angles of developed porous samples are shown in Fig. 26 and Fig. 27.

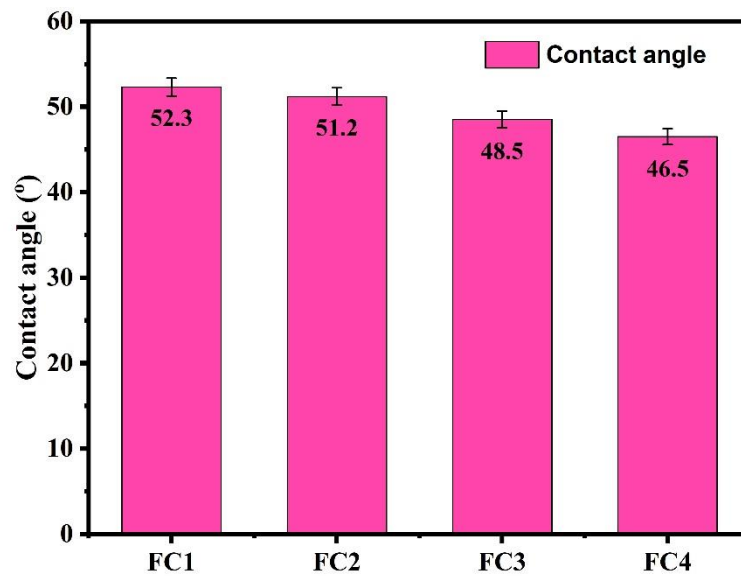


**Figure 26** Contact angle of developed porous alloys.

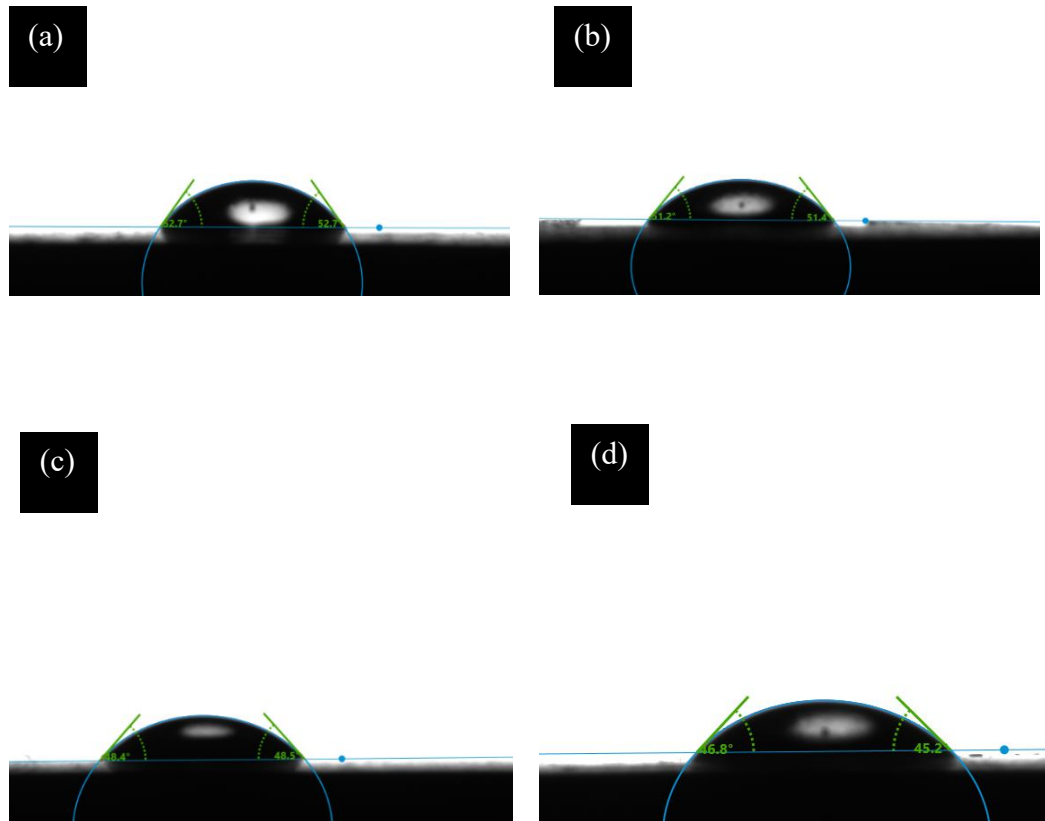


**Figure 27** Contact angle Developed porous alloys (a)FC1 (b) FC2 (c) FC3 (d) FC4

#### **4.7 Corrosion Results:**

The physiological environment within the human body differs significantly from the surroundings in terms of both physical and chemical aspects. As a result, a metal that performs well under normal environments, such as being inert or passive, may suffer significant corrosion when exposed to the inside environment of the body. When used in biomedical applications, a particular combination of biological fluids, pH levels, electrolyte presence, and other variables within the body can cause accelerated corrosion of metals, which can have negative impacts on the material's integrity and performance. To ensure long-term effectiveness and safety, compatibility and corrosion resistance must be considered during materials designing for their use within the human body for. To analyze the chemical stability of the porous alloys using a solution having an ionic concentration like human blood plasma electrochemical testing was carried out. The studies were conducted under specific environments, including a 37°C temperature, a pH of 7.4, and a three-electrode setup.

The purpose of these testing was to acquire a better understanding of how porosity influences the electrochemical characteristics and corrosion resistance of foams.

#### 4.7.1 Open Circuit Potential:

Open Circuit Potential (OCP) of porous samples was determined for a duration of 3600 seconds in shown Fig. 28. During the exposure period, a consistent shift in the Open Circuit Potential (OCP) towards greater negative values was noticed. This negative shift was always accompanied by a corresponding increase in total current. For FC1 foam open circuit potential reached a value of (-0.136V) after immersion in solution and remained stable for 3600 s. A negative shift in OCP was observed for FC2 to FC4, which is mainly due to an increase in porosity results in a increased surface area which in turn increase the oxide reactions on surface. Researchers Li et al. ,Blackwood et al. [121], and Xie et al. [118] have previously documented this type behaviour. Their research has shown that significant shift in potential is associated with increasing porosity.

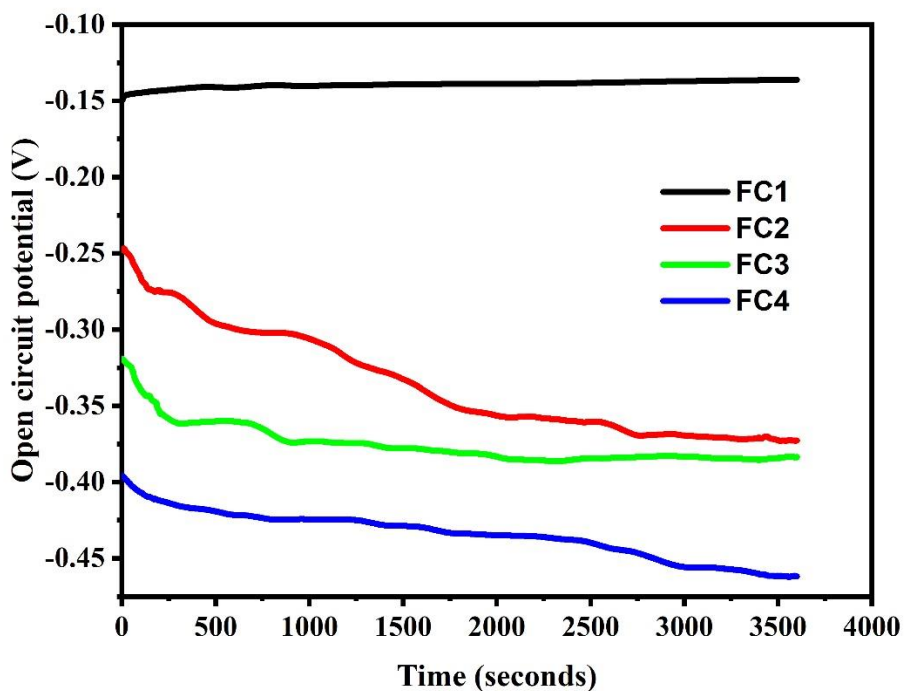


**Figure 28.** Open circuit potential vs time of developed porous alloys in hank's solution.

#### 4.7.2 Potentiodynamic polarization:

Porous samples were polarized and their behaviour was recorded under applied voltage. A significant increase in current density and a negative shift in corrosion potential was observed in all foams from FC1 to FC4. Passivation phenomena appeared in all of the foams investigated. This indicates that on the surface, a protective

oxide layer started to develop, contributing to their corrosion resistance. Despite being exposed to corrosive environments, the current density, which is related with the corrosion rate, remain almost stable. This shows that the protective oxide layer successfully slow down the progression of the corrosion processes. Passivation is the characteristic of titanium alloys which readily form titanium oxide layer on the surface when they exposed to body fluids[105]. In addition, no pitting features were found in curves for any of the foam samples. Pitting type of localised corrosion that is identified by the occurrence of small pits or holes on the material's surface. The lack of pitting behaviour in the foams suggests that they are resistant to this type of corrosion, which is often more damaging and can result in localized damage and material failure. Corrosion properties were measured by tafel plots on anodic and cathodic branches. FC1 show high resistance to corrosion in solution compared to other developed foams in this study. High corrosion resistance of FC1 among other foams is because it contains low porosity compared to others. FC4 showed high corrosion rate of due to higher amount of porosity resulting in enhanced surface area exposed in solution and available for oxidation higher the number of electrons generated, resulting in high current density. Fig. 29 shows the polarization curves of samples with porosity range 1.6 % to 7.36%. Variation in the corrosion parameters that is  $i_{corr}$ ,  $E_{corr}$  and corrosion rate is due to increased surface area exposed to solution.  $i_{corr}$ ,  $E_{corr}$  and corrosion rates are presented in the Table 6. below.

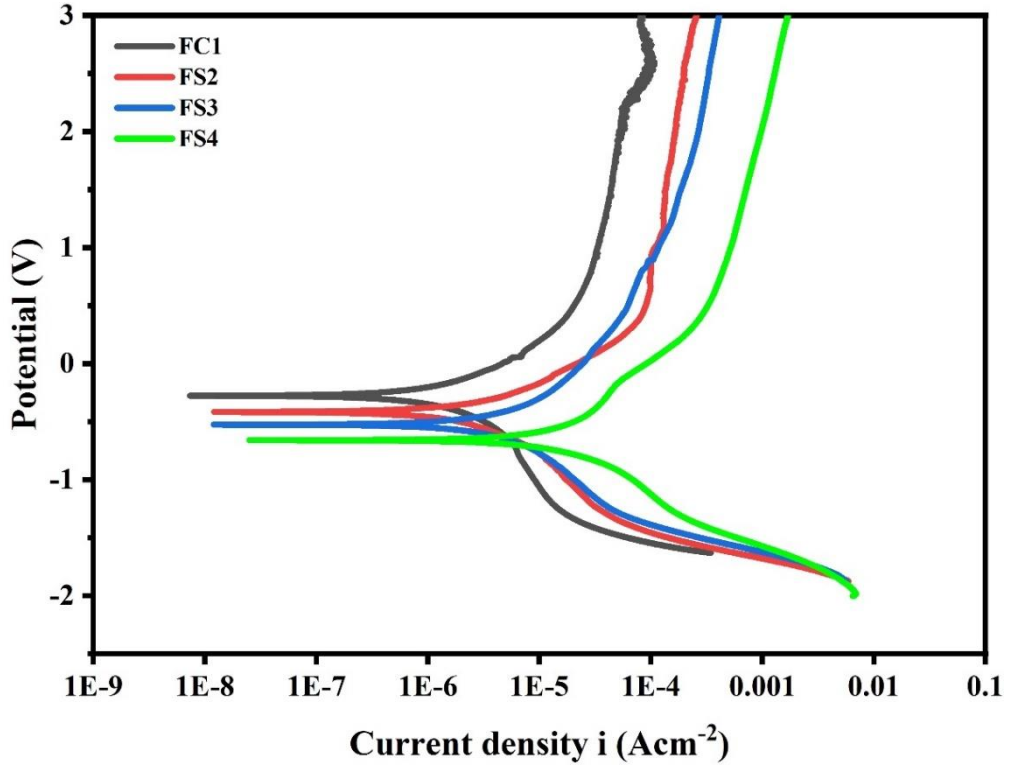


**Figure 29.** Electrochemical results of Developed foams being exposed to Hank's solution.

**Table 6** Corrosion parameters calculated from polarization curves and EIS.

	$i_{corr}$ ( $\mu\text{A}$ )	$E_{corr}$ (mV)	Corrosion rate (mpy)	OCP (mV)	$R_p$ (Kohm)
FC1	3.120	-277.0	1.929	-136.1	42.51
FC2	5.210	-417.2	3.342	-372.7	11.03
FC3	14.90	-526	9.083	-383.6	8.693
FC4	18.70	-660	12.65	-461.1	2.691



#### **4.7.3 Electrochemical impedance spectroscopy (EIS):**

Nyquist's plot of the porous alloys tested in Hank's solution are shown in the Fig. 30. Impedance was decreased for all samples. In Nyquist plot diameter of semi-circle represents the magnitude of impedance, FC1 exhibited the maximum impedance while FC4 showed less impedance. The polarization and corrosion resistance results are in agreement with the impedance measurements for all samples. FC1 showed higher corrosion resistance than the other samples, and also in Nyquist plots FC1 showed maximum resistance. The order of corrosion resistance calculated in polarization curves, was  $FC1 > FC2 > FC3 > FC4$ , the same order of corrosion resistance was observed in Nyquist plots. Here, in Nyquist plots, diameter of semicircle decreased from FC1 to FC4 showing a decrease in corrosion resistance with increase in percentage porosity shown in Fig (30).  $R_p$  represents the value of resistance at electrode and electrolyte interface. A high  $R_p$  value means less current leakage at the interface, which indicates improved corrosion resistance. The high  $R_p$  value of FC1 indicates a low current flow at the interface of FC1 and solution, indicating higher resistance to corrosion in hanks solution. FC2, FC3, and FC4 showed lower corrosion resistance than that of FC1, which is due to their low  $R_p$  values, indicates greater current flow at the interface.

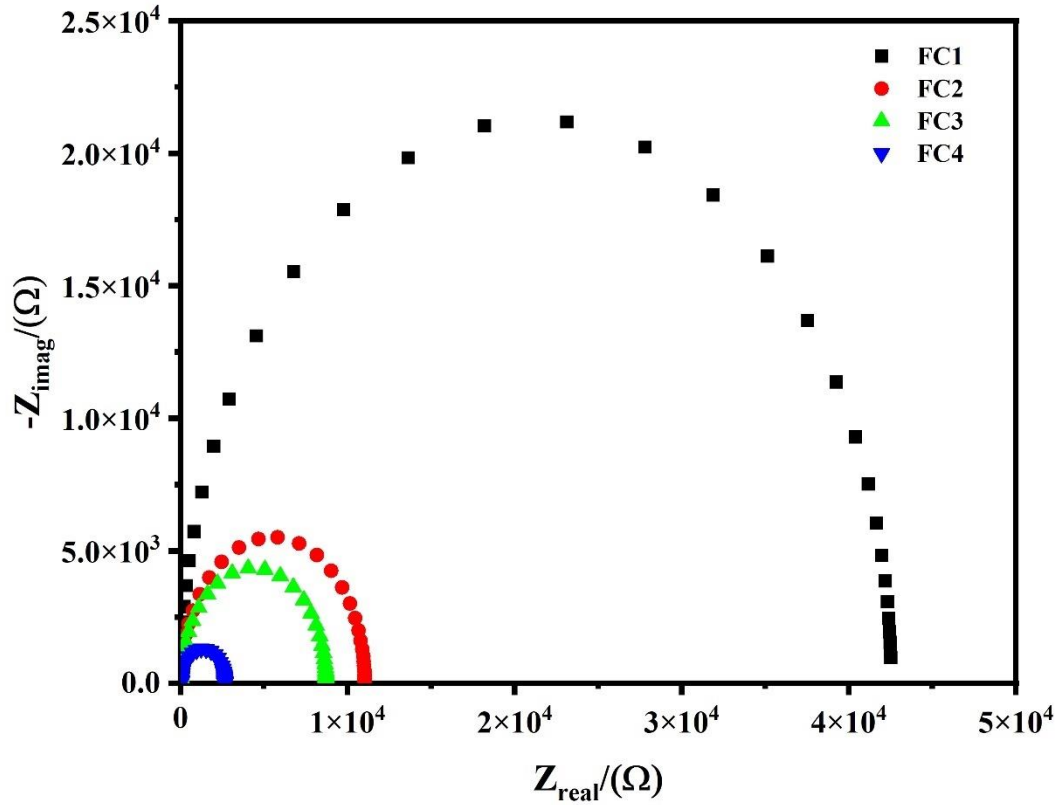


**Figure 30** Nyquist plot from Electrochemical Impedance of Porous Ti-35Nb-5Ta-7Zr alloys

The Ashby chart in Fig. 31 typically illustrates several materials or samples as scatter plots between  $E_{corr}$  and  $I_{corr}$ . The corrosion rate is shown by the  $I_{corr}$  readings, with values that are lower indicating less corrosion rates and better corrosion resistance. The  $E_{corr}$  values show the corrosion potential, with greater positive values indicating material's tendency to resist corrosion.

Developed porous samples indicated better corrosion resistance compared to other conventional and non-conventional porous materials. FC1 shows minimum  $i_{corr}$  value among all materials presented in the chart, showing better resistance against corrosion.

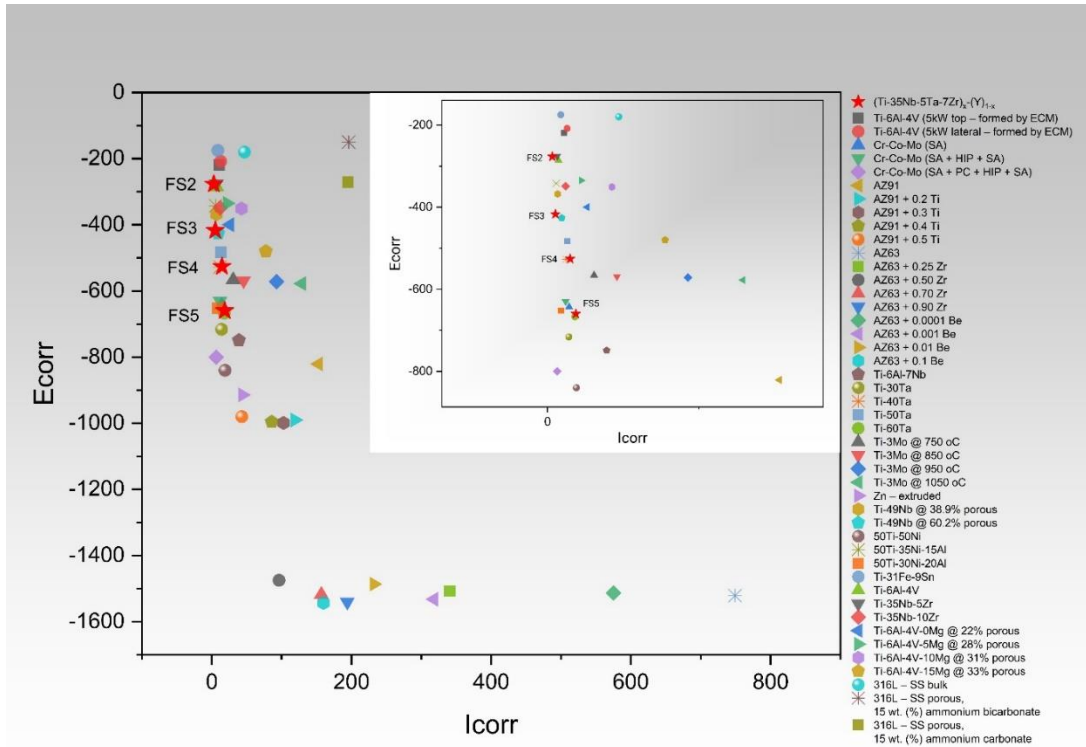


**Figure 31** Comparison of  $E_{corr}$  and  $I_{corr}$  value of porous alloys in this study with literature.

This comparison allows us to select materials based on better resistance. The  $I_{corr}$  and  $E_{corr}$  values of FC1 on the top left suggest that it's better corrosion resistant material than the stainless steel 316L Bulk, 316L porous, Cr-Co-Mo, Ti-6Al-V, Ti-6Al-7Nb, Ti-9Nb with 38.9% porosity and Ti-49Nb with 60.2% porosity. FC2, FC3 and FC4 with 4,6 and 8 % porosities have lower  $i_{corr}$  values than the stainless steel 316 Bulk and Porous and Ti-6Al-4V-0Mg with 22 and 28% porous materials. This analysis suggests that the foams developed in this study have better corrosion resistance in corrosion environment and have the potential to replace conventional implants.

## Conclusion

Foams were successfully manufactured through the addition of yttrium into a Ti-35Nb-5Ta-7Zr matrix via vacuum arc melting and subsequent chemical dealloying. The following are the investigation's principal findings:

- The inclusion of yttrium resulted in the production of interdendritic structures, which aided in the formation of interconnected 3D porosity during the chemical dealloying process.
- Mechanical testing was used to achieve and assess various levels of porosity.
- Under compression loadings Ti-35Nb-5Ta-7Zr foams had exceptional mechanical characteristics. The mechanical properties of the foams FC1, FC2, FC3 and FC4 showed elastic modulus was particularly in the elastic modulus range of bone along with high yield strength which is preferentially the requirement for implants.
- Mechanical and corrosion properties were evaluated which highlights the potential of developed porous alloys in orthopedic implants applications.

## References

- [1] Ronald Lakatos M. A. H., General Principles of Internal Fixation. Medscape 2018
- [2] Geetha M., Singh A. K., Asokamani R. and Gogia A. K. Ti based biomaterials, the ultimate choice for orthopaedic implants – A review. Progress in Materials Science 54(3) (2009), 397-425.
- [3] Aherwar A., Singh A. K. and Patnaik A. Current and future biocompatibility aspects of biomaterials for hip prosthesis. AIMS Bioeng 3(1) (2015), 23-43.
- [4] Aherwar A., Singh A. K. and Patnaik A. Cobalt Based Alloy: A Better Choice Biomaterial for Hip Implants. Trends in Biomaterials 30(1) (2016).
- [5] The state of musculoskeletal health 2019; Versus Arthritis
- [6] Tracey Loftis B. E., Tom Margham Musculoskeletal conditions and multimorbidity 2016.
- [7] Curtis E. M., van der Velde R., Moon R. J., van den Bergh J. P., Geusens P., de Vries F., van Staa T. P., Cooper C. and Harvey N. C. Epidemiology of fractures in the United Kingdom 1988–2012: variation with age, sex, geography, ethnicity and socioeconomic status. Bone 87 (2016), 19-26.
- [8] Sözen T., Özışık L. and Başaran N. Ç. An overview and management of osteoporosis. European journal of rheumatology 4(1) (2017), 46.
- [9] H.. Long, M., Rack, Titanium alloys in total joint replacement—a materials science perspective., Biomaterials. 19 (1998) 1621–1639.
- [10] Mehdizadeh M, Yang J. Design strategies and applications of tissue bioadhesives. Macromol Biosci 2013;13(3):27188.
- [11] Yoruc, ABH, Sener BC. Biomaterials. In: Prof. Kara S, editor. A roadmap of biomedical engineers and milestones; 2012, ISBN: 978-953-51-0609-8
- [12] Anderson JM. Biological responses to materials. Annu Rev Mater Res 2001; 31:81-110
- [13] Vallet-Regí M. Ceramics for medical applications. J Chem Soc Dalton Trans 2001;2:97-108.
- [14] Niinomi M. Recent metallic materials for biomedical applications. Metal Mater Trans A 2002;33 (3):477-86.
- [15] Bartolo P, Kruth J-P, Siva J, et al. Biomedical production of implants by additive electro-chemical and physical processes. CIRP Ann: Manuf Techn 2012; 61: 635–655.
- [16]. Williams DF. On the mechanisms of biocompatibility. Biomaterials 2008; 29: 2941–2953
- [17] H.. Long, M., Rack, Titanium alloys in total joint replacement—a materials science perspective., Biomaterials. 19 (1998) 1621–1639.
- [18] J.I. Qazi, H.J. Rack, Metastable beta titanium alloys for orthopedic applications, Adv. Eng. Mater. 7 (2005) 993–998. doi:10.1002/adem.200500060.

- [19] K. Wang, The use of titanium for medical applications in the USA, *Mater. Sci. Eng. A.* 213 (1996) 134–137. doi:10.1016/0921-5093(96)10243-4.
- [20] V. Sheremetyev, V. Brailovski, S. Prokoshkin, K. Inaekyan, S. Dubinskiy, Functional fatigue behavior of superelastic beta Ti-22Nb-6Zr(at%) alloy for load-bearing biomedical applications, *Mater. Sci. Eng. C.* 58 (2016) 935–944. doi:10.1016/j.msec.2015.09.060.
- [21]. Gittens RA, McLachlan T, Olivares-Navarrete R, et al. The effects of combined micron-/submicron-scale surface roughness and nanoscale features on cell proliferation and differentiation. *Biomaterials* 2011; 32: 3395–3403.
- [22] Sumner, D., et al., Functional adaptation and ingrowth of bone vary as a function of hip implant stiffness. (1998). 31(10): p. 909-917.
- [23] Rack, H.J. and J.I. Qazi, Titanium alloys for biomedical applications. *Materials Science and Engineering: C*, (2006). 26(8): p. 1269-1277.
- [24] Niinomi, M., M. Nakai, and J. Hieda, Development of new metallic alloys for biomedical applications. *Acta Biomaterialia*, (2012). 8(11): p. 3888-3903.
- [25] Teichtahl A. J., Wluka A. E., Wijethilake P., Wang Y., Ghasem-Zadeh A. and Cicuttini F. M. Wolff's law in action: a mechanism for early knee osteoarthritis. *Arthritis Research & Therapy* 17(1) (2015), 207
- [26] Malchau H. and Herberts P. Prognosis of total hip replacement: revision and re-revision rate in THR: a revision-risk study of 148,359 primary operations. 1998.
- [27] Ridzwan M. I. Z., Shuib S., Hassan A. Y., Shokri A. A. and Ibrahim M. N. M. Problem of stress shielding and improvement to the hip implant designs: a review. *J. Med. Sci* 7(3) (2007), 460-467.
- [28] Denard P. J., Raiss P., Gobezie R., Edwards T. B. and Lederman E. Stress shielding of the humerus in press-fit anatomic shoulder arthroplasty: review and recommendations for evaluation. *Journal of shoulder and elbow surgery* 27(6) (2018), 1139-1147
- [29] Teles A. R., Yavin D., Zafeiris C. P., Thomas K. C., Lewkonja P., Nicholls F. H., Swamy G. and Jacobs W. B. Fractures After Removal of Spinal Instrumentation: Revisiting the Stress-Shielding Effect of Instrumentation in Spine Fusion. *World neurosurgery* 116 (2018), e1137-e1143
- [30] Malchau H., Herberts P. and Ahnfelt L. Prognosis of total hip replacement in Sweden: follow-up of 92,675 operations performed 1978–1990. *Acta Orthopaedica Scandinavica* 64(5) (1993), 497-506.
- [31] *Mettalic materials*, J.R. Davies (Ed.), Handbook of Materials for Medical Devices, ASM International, Materials Park, Ohio, 2003, pp. 21–50.
- [32] D.W. Lennox, B.H. Schofield, D.F. McDonald, L.H. Riley, *Clin. Orthop.* (1987) 171–191
- [33] A. Doran, F.C. Law, M.J. Allen, N. Rushton, *Biomaterials* 19 (1998) 751–759

- [34] M. Sumita, T. Hanawa, Failure processes in biometallic materials, *Bioengineering*, vol. 9, Elsevier Science Ltd., London, 2003, pp. 131–167
- [35] K. Nakazawa, M. Sumita, N. Maruyama, *Jpn. Inst. Met.* 63 (1999) 1600–1608.
- [36] K. Nakazawa, M. Sumita, N. Maruyama, Fatigue and fretting fatigue of austenitic and ferritic stainless steels in pseudo-body fluid, in: *Fatigue'99: Proceedings of the 7th International Fatigue Congress, Beijing (P.R. China), 8–12 June, 1999*, X.R. Wu (Ed.), EMAS Publishing, vol. 2, pp. 1359–1364
- [37] Q.Z. Chen, D.M. Knowles, *Mater. Sci. Eng. A* 356 (2003) 352–367
- [38] S. Pramanik, A.K. Agarwal, K.N. Rai, *Trends Biomater. Artif. Organs* 19 (2005) 15–26.
- [39] M. Navarro, A. Michiardi, O. Castan˜o, J.A. Planell, *J. R. Soc. Int.* 5 (2008) 1137–1158.
- [40] H.J. Raithel, K.H. Schaller, *Zentralbl. Bakteriolog.* 173 (1981) 63–91.
- [41] J.J. Ramsden, D.M. Allen, D.J. Stephenson, J.R. Alcock, G.N. Peggs, G. Fuller, G. Goch, *CIRP Ann. Manuf. Technol.* 56 (2007) 687–711.
- [42] O. Ozturk, U. Turkkan, A.E. Eroglu, *Surf. Coat. Technol.* 200 (2006) 5687–5697.
- [43] C.V. Vidal, A.I. Mun˜oz, *Electrochim. Acta* 54 (2009) 1798–1809.
- [44] G.L. (Gerd), J.C.W.J. Case, *Titanium*, Springer, New York, 2003.
- [45] A. Biesiekierski, D.H. Ping, Y. Yamabe-Mitarai, C. Wen, *Mater. Des.* 59 (2014) 303–309
- [46] I. Pais, M. Feher, E. Farkas, Z. Szabo, I. Cornides, *Commun. Soil Sci. Plant Anal.* 8 (1977) 407–410.
- [47] S. Yaghoubi, C.W. Schwietert, J.P. McCue, *Biol. Trace Elem. Res.* 78 (2000) 205–217.
- [48] M.L. Wang, R. Tuli, P.A. Manner, P.F. Sharkey, D.J. Hall, R.S. Tuan, *J. Orthop. Res.* 21 (2003) 697–707.
- [49] N. Coen, M.A. Kadhim, E.G. Wright, C.P. Case, C.E. Mothersill, *Br. J. Cancer* 88 (2003) 548–552.
- [50] R. Kumazawa, F. Watari, N. Takashi, Y. Tanimura, M. Uo, Y. Totsuka, *Biomaterials* 23 (2002) 3757–3764
- [51] V.V. Koval'skii, L.T. Rezaeva, *Usp. Sovrem. Biol.* 60 (1965) 45–61.
- [52] E.P. Daniel, E.M. Hewston, *Am. J. Physiol.* 136 (1942) 0772–0775.
- [53] M.A. Altamirano-Lozano, M.E. Roldan-Reyes, E. Rojas, *Vanadium in the Environment, Pt. 2: Health Effects*, vol. 31, 1998, pp. 159–179.

- [54] L.S. Rhoads, W.T. Silkworth, M.L. Roppolo, M.S. Whittingham, *Toxicol. In Vitro* 24 (2010) 292–296.
- [55] N.B. Ressa, B.J. Chou, R.A. Renne, J.A. Dill, R.A. Miller, J.H. Roycroft, J.R. Hailey, J.K. Haseman, J.R. Bucher, *Toxicol. Sci.* 74 (2003) 287–296.
- [56] B. Moretti, V. Pesce, G. Maccagnano, G. Vicenti, P. Lovreglio, L. Soleo, P. Apostoli, *Lancet* 379 (2012) 1676.
- [57] S.V. Verstraeten, L. Aimo, P.I. Oteiza, *Arch. Toxicol.* 82 (2008) 789–802.
- [58] J.E. Lemons, K.M.W. Niemann, A.B. Weiss, *J. Biomed. Mater. Res.* 10 (1976) 549–553
- [59] T. Kodama, *Kokubyo Gakkai zasshi, J. Stomatol. Soc. Jpn.* 56 (1989) 263–288.
- [60] M. Niinomi, *Mater. Trans.* 49 (2008) 2170–2178.
- [61] M. Niinomi, *Metall. Mater. Trans. A* 33 (2002) 477–486
- [62] G. Lu`tjering, J.C. Williams, *Titanium*, Springer, Berlin, 2007.
- [63] V.D. Cojocaru, D. Raducanu, I. Cinca, I. Dan, S. Ivanescu, E. Jalba, *Metal. Int.* 16 (2011) 35–38.
- [64] D. Raducanu, E. Vasilescu, V.D. Cojocaru, I. Cinca, P. Drob, C. Vasilescu, S.I. Drob, *J. Mech. Behav. Biomed. Mater.* 4 (2011) 1421–1430.
- [65] Y.X. Tong, B. Guo, Y.F. Zheng, C.Y. Chung, L.W. Ma, *J. Mater. Eng. Perform.* 20 (2011) 762–766
- [66] P.J. Bania, in: D. Eylon, R.R. Boyer, D.A. Koss (Eds.), *Titanium Alloys in the 1990's*, The Mineral, Metals & Materials Society, Warrendale, PA, 1993, pp. 3–14.
- [67] R.W. Schutz, in: D. Eylon, R.R. Boyer, D.A. Koss (Eds.), *Beta Titanium Alloys in the 1990's*, The Mineral, Metals & Materials Society, Warrendale, PA, 1993, pp. 75–91.
- [68] K.L. Wapner, "Implications of metallic corrosion in total knee arthroplasty", *Clin. Orthop. Relat. Res.*, Vol. 271, p.12-20, 1991.
- [69] D.M. Gordina, T. Glorianta, G. Nemtoib, "Synthesis, structure and electrochemical behavior of a beta Ti-12Mo-5Ta alloy as new biomaterial", *Mater. Lett.*, Vol. 59, pp.2959, 2005.
- [70] S. Tamilselvi, V. Raman, and N. Rajendran, "Corrosion behaviour of Ti 6Al-7Nb and Ti-6Al-4V ELI alloys in the simulated body fluid solution by electrochemical impedance spectroscopy", *Electrochim. Acta*, Vol. 52, p.839, 2006.
- [71] Y. Okazaki, Y. Ito, T. Tateishi, A. Ito, "Effect of heat treatment on microstructure and mechanical properties of new titanium alloys for surgical implantation", *J 834 Jpn Inst Met*, Vol. 59, pp.108–115, 1995
- [72] CRM. Afonso, GT. Aleixo, AJ. Ramirez, R. Caram, "Influence of cooling rate on microstructure of Ti–Nb alloy for orthopedic implants", *Mater Sci Eng C*, Vol.889, pp.908–913, 2007.



- [73] LD. Zardiackas, DW. Mitchell, JA. Disegi, "Characterization of Ti–15Mo Beta Titanium Alloy for Orthopedic Implant", In: Brown SA, Lemons JE, editors, *Medical applications of titanium and its alloys*, ASTM STP 1272. West Conshohocken, PA: ASTM International, pp. 60–75, 1996
- [74] Xingfeng Zhao, M. Niinomi, Masaaki Nakai, Junko Hieda, "Beta type Ti–Mo alloys with changeable Young's modulus for spinal fixation applications, *Acta Biomaterialia*, Vol. 8, pp. 1990–1997, 2012.
- [75] YL. Zhou and M. Niinomi, "Ti-25Ta alloy with the best mechanical compatibility in Ti-Ta alloys or bio- medical applications," *Materials Science and Engineering: C*, Vol. 29, pp. 1061-1065, 2009.
- [76] WF Ho, WK Chen, SC Wu, " Hsu HC. Structure, mechanical properties, and grindability of dental Ti–Zr alloys", *J Mater Sci Mater Med*, Vol. 19, pp.3179–86, 2008.
- [77] Ikeda M, Ueda M, Matsunaga R, Ogawa M, Niinomi M., "Isothermal aging behavior of beta titanium–manganese alloys", *Mater Trans*, Vol. 50, pp. 2737–43, 2009.
- [78] M. Nakai, M. Niinomi, XF. Zhao, XL. Zhao, "Self-adjustment of Young's modulus in biomedical titanium alloy during orthopaedic operation", *Mater Lett* 2, 2011.
- [79] WF Ho, TY Chiang, SC Wu, HC Hsu, "Mechanical properties and deformation behavior of cast binary Ti–Cr alloys", *J Alloy Compd*, Vol.. 468, pp. 533–538, 2009.
- [80] Y. Al-Zain, HY. Kim, H. Hosoda, TH. Nam, S. Miyazaki, "Shape memory properties of Ti–Nb–Mo biomedical alloys", *Acta Mater*, Vol.58, pp.4212–4223, 2010.
- [81] D. Ping, Y. Mitarai, F. Yin, "Microstructure and shape memory behavior of a Ti–30Nb–3Pd alloy", *Scripta Mater*, Vol.52, pp.1287–1291, 2005.
- [82] AK Mishra, JA Davidson, RA Poggie, P Kovacs, TJ Fitzgerald, *Mechanical and Tribological Properties and Biocompatibility of Diffusion Hardened Ti–13Nb–13Zr – A New Titanium Alloy for Surgical Implants*, In: Brown SA, Lemons JE, editors. *Medical Applications of Titanium and its Alloys*, ASTM STP. West Conshohocken, PA: ASTM International; 1996. p. 96–116.
- [83] L.W. Ma, H.S. Cheng, C.Y. Chung, "Effect of thermo-mechanical treatment on superelastic behavior of Ti-19Nb-14Zr (at%) shape memory alloy", *Intermetallic*, Vol. 32, pp. 44-50, 2013.
- [84] K. Miura, N. Yamada, S. Hanada, TK. Jung, E. Itoi, "The bone tissue compatibility of a new Ti–Nb–Sn alloy with a low Young's modulus", *Acta Biomater*, Vol.7, pp.2320–2326, 2011.
- [85] H.Y. Kim, S. Hashimoto, J.I. Kim, T. Inamura, H. Hosoda, S. Miyazaki, " Effect of Ta addition on shape memory behavior of Ti–22Nb alloy", *Materials Science and Engineering A*, Vol. 417, pp. 120–128, 2006.

- [86] J. Málek, J.F. Hnilica, J. Vesely, B. Smola, S. Bartakova, J. Vanék, "The influence of chemical composition and thermo-mechanical treatment on Ti–Nb–Ta alloys", *Mater Des*, Vol.35, pp.731–740, 2012.
- [87] Hsueh-Chuan Hsu, Shih-Kuang Hsu, Shih-Ching Wu, Chih-Jhan Leec, Wen-Fu Ho, " Structure and mechanical properties of as-cast Ti–5Nb–xFe alloys", *Materials Characteristics*, Vol. 61, pp. 851-858, 2010.
- [88] DP. Cao, "Mechanical and electrochemical characterization of Ti–12Mo–5Zr alloy for biomedical application", *J. Alloys Compd*, Vol.509, pp.8235–8238, 2011.
- [89] S.B. Gabriel, J.V.P. Panaino, I.D. Santos, L.S. Araujo, P.R. Mei, L.H. de Almeida, C.A. Nunes, " Characterization of a new beta titanium alloy, Ti–12Mo–3Nb, for biomedical applications", *Journal of Alloys and Compounds*, 2011.
- [90] M. Ikeda, D. Sugano, "The effect of aluminum content on phase constitution and heat treatment behavior of Ti–Cr–Al alloys for healthcare applications", *Mater Sci Eng C*, Vol. 25, pp. 377–381, 2005.
- [91] S. Hatanaka, M. Ueda, M. Ikeda, M. Niinomi, "Isothermal aging behavior in Ti–10Cr–Al alloys for medical applications", *Adv Mater Res*2010;89–91:232–7.
- [92] Ljerka Slokar, Tanja Matkovic, Prosper Matkovic, "Alloy design and property evaluation of new Ti–Cr–Nb alloys", *Materials and Design*, Vol.33, pp.26–30, 2012.
- [93] A. Wadood, T.Inamura, Y.Yamabe-Mitarai, H.Hosoda, "Strengthening of b Ti–6Cr–3Sn alloy through b grain refinement, a phase precipitation and result in effect on shape memory properties", *Materials Science & Engineering A*, Vol. 559, pp. 829–835, 2013.
- [94] Ikeda M, Ueda M, Matsunaga R, Niinomi M. Phase constitution and heat treatment behavior of Ti–7 mass %Mn–Al alloys. *Mater Sci Forum* 654– 656, pp. 855–858, 2010.
- [95] E. Bertrand, T. Gloriant, D.M. Gordin, E. Vasilescu, P. Drob, C. Vasilescu, S.I. Drob, " Synthesis and characterisation of a new superelastic Ti–25Ta–25Nb biomedical alloy", *J. mechanical behavior of biomedical materials*, vol. 3, pp. 559-564, 2010.
- [96] Y.X. Tong, B. Guo, Y.F. Zheng, C.Y. Chung, and L.W. Ma, " Effects of Sn and Zr on the Microstructure and Mechanical Properties of Ti-Ta Based Shape Memory Alloys", *JMEPEG*, Vol. 20, pp. 762–766, 2011.
- [97] M. Ikeda, M. Ueda, T. Kinoshita, M. Ogawa, M. Niinomi, " Influence of Fe content of Ti–Mn–Fe alloys on phase constitution and heat treatment behavior", *Mater Sci Forum*, Vol. 706–709:1893–1898, 2012.
- [98] S. Ashida, H. Kyogaku, H. Hosoda, "Fabrication of Ti–Sn–Cr shape memory alloy by PM and its properties", *Mater Sci Forum*, Vol. 706–709, pp. 1943–7, 2012.
- [99] M. Ikeda, S. Komatsu, Y. Nakamura, "Effects of Sn and Zr additions on phase constitution and aging behavior of Ti–50 mass%Ta alloys quenched from  $\beta$  single phase region", *Mater Trans*, Vol. 45, pp. 1106–1112, 2004.

- [100] YL. Hao, SJ. Li, SY. Sun, CY. Zheng, R. Yang, "Elastic deformation behaviour of Ti–24Nb–4Zr–7.9Sn for biomedical applications", *Acta Biomater*, Vol. 3, pp. 277–286, 2007.
- [101] Z. Guo, J. Fu, YQ. Zhang, YY. Hu, ZG. Wu, L. Shi, M. Sha, SJ. Li, YL. Hao, R. Yang, "Early effect of Ti–24Nb–4Zr–7.9Sn intramedullary nails on fractured bone", *Mater Sci Eng C*, Vol.29, pp.963–968, 2009.
- [102] WF. Cui, AH. Guo, "Microstructure and properties of biomedical TiNbZrFe  $\beta$ -titanium alloy under aging conditions", *Mater Sci Eng A*, Vol.527, pp.258–262, 2009.
- [103] P. Majumdar, S.B. Singh, M. Chakraborty, " Elastic modulus of biomedical titanium alloys by nano-indentation and ultrasonic techniques—A comparative study", *Materials Science and Engineering A*, Vol. 489, pp. 419–425, 2008.
- [104] Liqiang Wang, Weijie Lu, Jining Qin, Fan Zhang, Di Zhang, "Effect of precipitation phase on microstructure and superelasticity of cold-rolled beta titanium alloy during heat treatment", *Materials and Design*, Vol. 30, pp. 3873–3878, 2009.
- [105] Q. Wei, L. Wang, Y. Fu, J. Qin, W. Lu, D. Zhang, " Influence of oxygen content on microstructure and mechanical properties of Ti–Nb–Ta–Zr alloy", *Mater Des*, Vol.32, pp.2934–2939, 2011.
- [106] KK..Wang, LJ. Gustavson, JH. Dumbleton, "Microstructure and Properties of A New Beta Titanium Alloy, Ti–12Mo–6Zr–2Fe, Developed for Surgical Implants", In: Brown SA, Lemons JE, editors, *Medical Applications of Titanium and its Alloys*, ASTMSTP 1272. West Conshohocken, PA: ASTM International, pp.76–87, 1996.
- [107] D. Kuroda, H. Kawasaki, S. Hiromoto, T. Hanawa, "Development of new Ti–Fe–Ta and Ti–Fe–Ta–Zr system alloys for biomedical applications", *Mater Sci Eng C*, Vol.25, pp.312–320, 2005.
- [108] Y. Kasano, T. Inamura, H. Kanetaka, S. Miyazaki, H. Hosoda, "Phase constitution and mechanical properties of Ti–(Cr, Mn)–Sn biomedical alloys", *Mater Sci Forum*, Vol.654–656, pp.2118–2121, 2010.
- [109] E. Bertrand, T. Gloriant, D.M. Gordin, E. Vasilescu, P. Drob, C. Vasilescu, S.I. Drob, " Synthesis and characterisation of a new superelastic Ti–25Ta–25Nb biomedical alloy", *J. the mechanical behavior of biomedical materials*, Vol. 3, pp. 559–564, 2010
- [110] Changli Zhaoa, Xiaonong Zhanga, Peng Cao, Mechanical and Electrochemical Characterization of Ti–12Mo–5Zr Alloy for Biomedical Application, *Journal of Alloys and Compounds*, Vol. 509, pp.8235– 8238, 2011.
- [111]. Levine, B. (2008). A new era in porous metals: applications in orthopaedics. *Advanced Engineering Materials*, 10(9), 788-792.
- [112] Otsuki, B.; Takemoto, M.; Fujibayashi, S.; Neo, M.; Kokubo, T.; Nakamura, T. Pore throat size and connectivity determine bone and tissue ingrowth into porous implants: Three-dimensional micro-CT based structural analyses of porous bioactive titanium implants. *Biomaterials* 2006, 27, 5892–5900.
- [113] Mastrogiacomo, M.; Scaglione, S.; Martinetti, R.; Dolcini, L.; Beltrame, F.; Cancedda, R.; Quarto, R. Role of scaffold internal structure on in vivo bone formation in macroporous calcium phosphate bioceramics. *Biomaterials* 2006, 27, 3230–3237.

- [114] Habibovic, P.; Yuan, H.; van der Valk, C. M.; Meijer, G.; van Blitterswijk, C. A.; de Groot, K. 3D microenvironment as essential element for osteoinduction by biomaterials. *Biomaterials* 2005, 26, 3565–3575.
- [115] C.E. Wen, M. Mabuchi, Y. Yamada, K. Shimojima, Y. Chino, T. Asahina, *Scr. Mater.* 45 (2001) 1147–1153.
- [116] C.E. Wen, Y. Yamada, P.D. Hodgson, *Mater. Sci. Eng., C* 26 (2006) 1439–1444
- [117] Wang, X., Li, Y., Xiong, J., & Hodgson, P. D. (2009). Porous TiNbZr alloy scaffolds for biomedical applications. *Acta biomaterialia*, 5(9), 3616-3624.
- [118] Kotan, G., & Bor, A. Ş. (2007). Production and characterization of high porosity Ti-6Al-4V foam by space holder technique in powder metallurgy. *Turkish Journal of Engineering and Environmental Sciences*, 31(3), 149-156.
- [119]. Maya, A.E.A., et al., Zr–Ti–Nb porous alloys for biomedical application. *Materials Science and Engineering: C*, 2012. 32(2): p. 321-329.
- [120] Pałka, K. and R. Pokrowiecki, *Porous Titanium Implants: A Review. Advanced Engineering Materials*, 2018. 20(5).
- [121] Taddei, E.B., et al., Properties of Porous Ti-35Nb-7Zr-5Ta Processed by the Spacer Method for Use in Biomedical Applications. *Materials Science Forum*, 2008. 591-593: p. 224-229.
- [122] Rushdi, N.M.F.M., et al., Correlation between porosity and space holder content at different sintering temperatures of aluminum foam. 2016.
- [123] Singh, S. and N. Bhatnagar, A survey of fabrication and application of metallic foams (1925–2017). *Journal of Porous Materials*, 2017. 25(2): p. 537-554.
- [124] Parveez, B., et al., Microstructure and Mechanical Properties of Metal Foams Fabricated via Melt Foaming and Powder Metallurgy Technique: A Review. *Materials*, 2022. 15(15).
- [125] Han, Q., et al., Porous Tantalum and Titanium in Orthopedics: A Review. *ACS Biomater Sci Eng*, 2019. 5(11): p. 5798-5824.
- [126] Yang, K., et al., Additive manufacturing of in-situ reinforced Ti–35Nb–5Ta–7Zr (TNTZ) alloy by selective electron beam melting (SEBM). *Journal of Alloys and Compounds*, 2020. 826.
- [127] Guo, S., et al., Design and fabrication of a metastable beta-type titanium alloy with ultralow elastic modulus and high strength. *Sci Rep*, 2015. 5: p. 14688.
- [128] Rotta, G., T. Seramak, and K. Zasińska, Estimation of Young's Modulus of the Porous Titanium Alloy with the Use of Fem Package. *Advances in Materials Science*, 2015. 15(4): p. 29-37.
- [129] Han-Cheol, C. H. O. E., & Yeong-Mu, K. O. (2009). Mechanical properties and corrosion resistance of low rigidity quaternary titanium alloy for biomedical applications. *Transactions of Nonferrous Metals Society of China*, 19(4), 862-865.

[130] Mohammed, M. T., Khan, Z. A., & Siddiquee, A. N. (2014). Beta titanium alloys: the lowest elastic modulus for biomedical applications: a review. *Int. J. Chem. Mol. Nucl. Mater. Metall. Eng.* 8(8), 726-731.